Supporting Information

Structure–Property Relationships in Chalcones with Extended π-Conjugation: ICT Perturbation and Far-Red Fluorescence

Brian Corbin, Paityn Houglan, Wei-Yuan Chen, Christopher J. Ziegler, Yi Pang*

Department of Chemistry, The University of Akron, Akron, OH 44325-3601

Table of Content **Page number**

Experimental details for Mass Spectrometry Study. Mass spectrometry analysis was performed using a timsTOF Pro 2 Q/ToF (Bruker Billerica, MA), equipped with an electrospray ionization (ESI) source with an average mass resolving power of 50,000 FWHM (full width at half maximum). Stock samples were delivered dissolved into acetonitrile (ACN) to a concentration between 1-2 mg/mL. Before mass spectrometry analysis, the samples were filtered using Acrodisc 13 mm 0.2 μm PTFE filters followed via serial dilutions using ACN to a concentration between 20-100 ng/mL. The sample was then injected into the instrument via direct injection using a 1 mL syringe. The samples were ionized by ESI under the following optimized conditions. The mass range was set to m/z 50-500 at a rate of 1 Hz and MS averaging set to 1. The end plate offset, capillary voltage, nebulizer gas, dry gas, and dry temp were set to 400 V, 4000 V, 1.5 mbar, 4 L/min, and 150 °C, respectively. The polarity of the timsTOF was set to positive mode. For positive mode mass calibration, the calibrant solution used was ESI-L Low Concentration Tuning Mix (Tune Mix) and was obtained from Agilent Technologies (Santa Clara, CA). Before infusion into the mass spectrometer, the Tune Mix was diluted using a 1:1 mixture of acetonitrile and water, both Optima LC/MS grade, and were purchased from Fisher Scientific (Fair Lawn, NJ). All mass spectral data were collected using timsControl (Billerica, MA) and analyzed using Compass DataAnalysis (Billerica, MA) software. Peak processing parameters used the Sum Peak algorithm and the parameters are as follows: S/N threshold 10, Relative intensity threshold 0.1 %, the Absolute intensity threshold 100%, and Background Subtract Analysis Mode set to Xpose with a retention time window of +/- 0.5 s and a ratio of 5.

Synthesis of chalcones 1a-1f

Chalcone **1a** ((2E,4E)-5-(4-(dimethylamino)phenyl)-1-phenylpenta-2,4-dien-1-one): Acetophenone (1.1 mmol) and 4-(dimethylamino)cinnamaldehyde (1 mmol) were combined in ethanol (5 mL) in a 50 mL round-bottom flask and stirred for 5 min. Pyrrolidine (0.10 mL) was then added dropwise, and the reaction mixture was stirred at room temperature for 18 h. Upon completion, the reaction mixture was poured into ice–water (120 mL) and adjusted to pH ~6. The resulting mixture was extracted with dichloromethane (3 × 30 mL), and the combined organic layers were concentrated under reduced pressure. The crude products were purified by column chromatography on silica gel using dichloromethane as the eluent to afford **1a** as a crimson red solid in 81% yield.

Chalcone **1b** ((2E,4E)-1-(2-methoxyphenyl)-5-(4-(dimethylamino)phenyl)penta-2,4-dien-1-one): Same procedure as **1a** except 2-methoxyacetophenone was used instead of acetophenone. Chalcone **1b** was isolated as an orange-red solid in 84% yield.

Chalcone **1c** ((2E,4E)-1-(4-methoxyphenyl)-5-(4-(dimethylamino)phenyl)penta-2,4-dien-1-one: Same procedure as **1a** except 4-methoxyacetophenone was used instead of acetophenone. Chalcone **1c** was isolated as an orange solid in 80% yield.

Chalcone **1d** ((2E,4E)-1-(2,4-dimethoxyphenyl)-5-(4-(dimethylamino)phenyl)penta-2,4-dien-1-one: Same procedure as **1a** except 2,4-dimethoxyacetophenone was used instead of acetophenone. Chalcone **1d** was isolated in 78% yield as a red solid.

Chalcone **1e** ((2E,4E)-1-(2,6-dimethoxyphenyl)-5-(4-(dimethylamino)phenyl)penta-2,4-dien-1-one): Same procedure as **1a** except 2,6-dimethoxyacetophenone was used instead of acetophenone. Chalcone **1e** was isolated in 74% yield as an orange solid.

Chalcone **1f** ((2E,4E)- 1-(2,4,6-trimethoxyphenyl)-5-(4-(dimethylamino)phenyl)penta-2,4-dien-1-one): Same procedure as **1a** except 2,4,6-trimethoxyacetophenone was used instead of acetophenone. Chalcone **1f** was isolated as an orange solid in 75% yield.

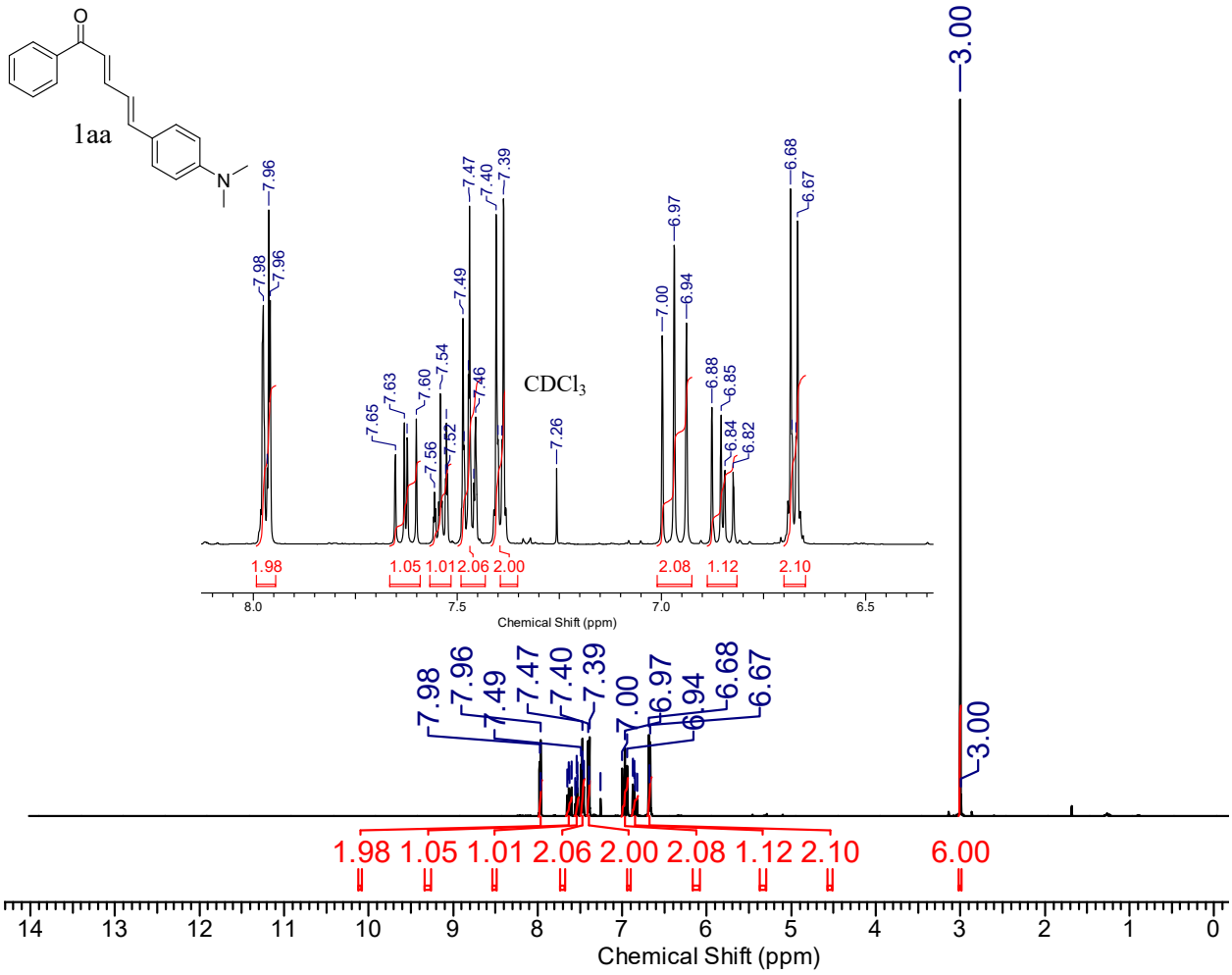

Figure S1. ^{1}H NMR of **1a** (500MHz, $CDCl_3$) δ 7.98-7.96 (d, J = 6.85 Hz, 2H), 7.65-7.60 (dd, J = 14.48, 10.76 Hz 1H), 7.56-7.53 (t, J = 7.34 Hz, 1H), 7.49-7.46 (m, 2H), 7.40-7.39 (d, J = 8.80 Hz, 2H), 7.00-6.94 (t, J = 14.67 Hz, 2H), 6.88-6.82 (dd, J = 14.71, 10.27 Hz, 1H), 6.68-6.67 (d, J = 8.80 Hz, 2H), 3.00 (s, 6H, NMe_2).

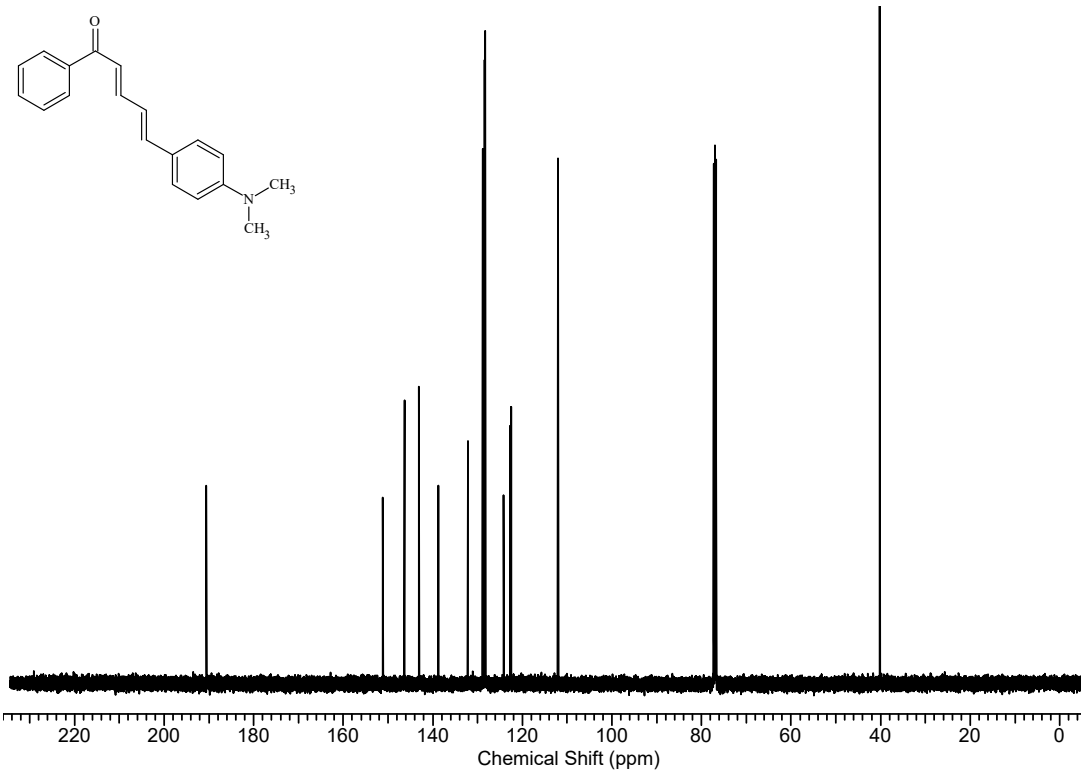

Figure S2. ^{13}C NMR of **1a** (125 MHz, $CDCl_3$) δ 190.5, 151.1, 146.4, 143.1, 138.8, 132.2, 128.9, 128.4, 128.3, 124.2, 122.7, 122.5, 112.0, 40.2 ppm.

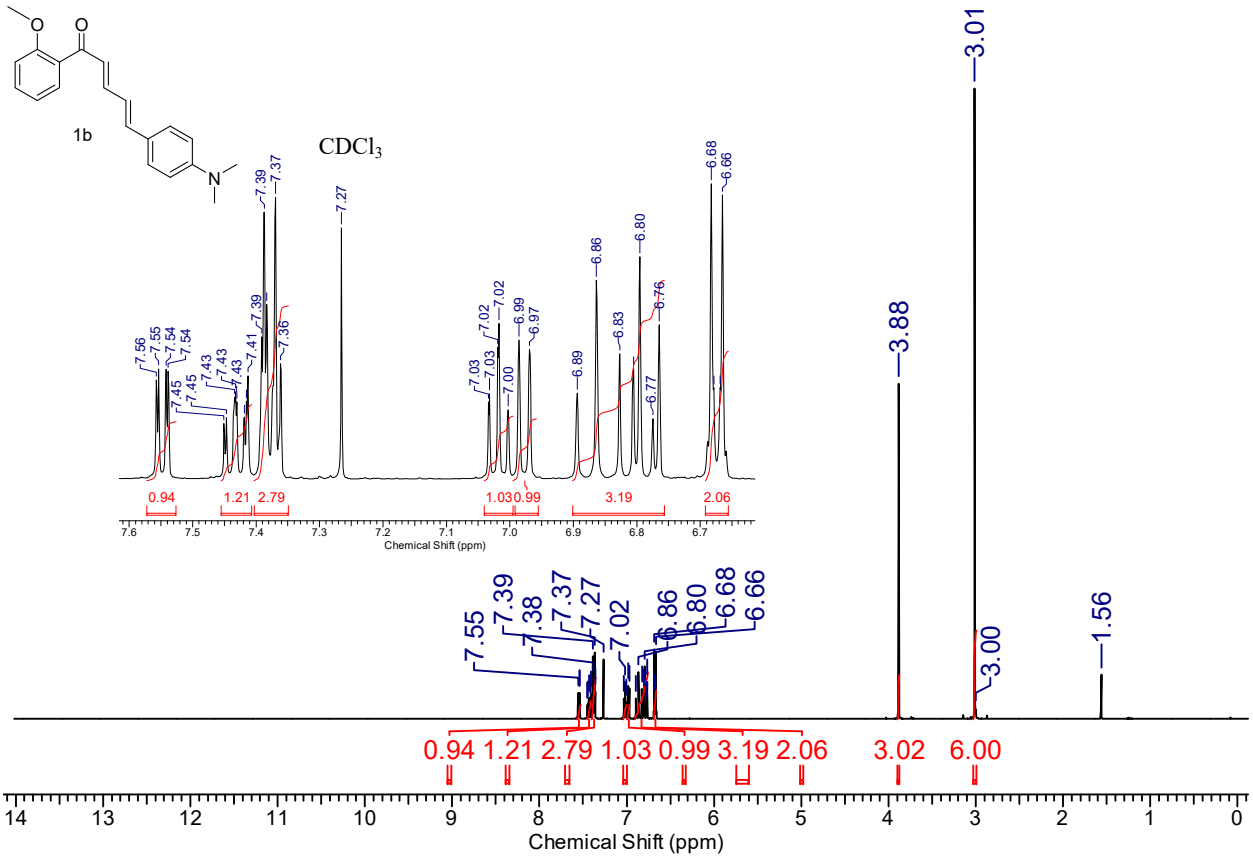

Figure S3. [1]HNMR of **1b** (500MHz, $CDCl_3$). δ 7.55 (dd, J = 7.5, 1.8 Hz,1H), 7.45-7.37 (m, 4H), 7.02 (td, J = 7.5, 1.1 Hz, 1H), 6.98 (d, 8.1 Hz, 1H), 6.87 (d, J = 15.5 Hz, 1H), 6.83-6.80 (d, J = 15.5 Hz, 1H), 6.81-6.78 (d, J = 15.1 Hz, 1H), 6.67 (d, J = 10 Hz, 2H), 3.88 (s, 3H, OCH3), 3.01 (s, 6H, NMe_2).

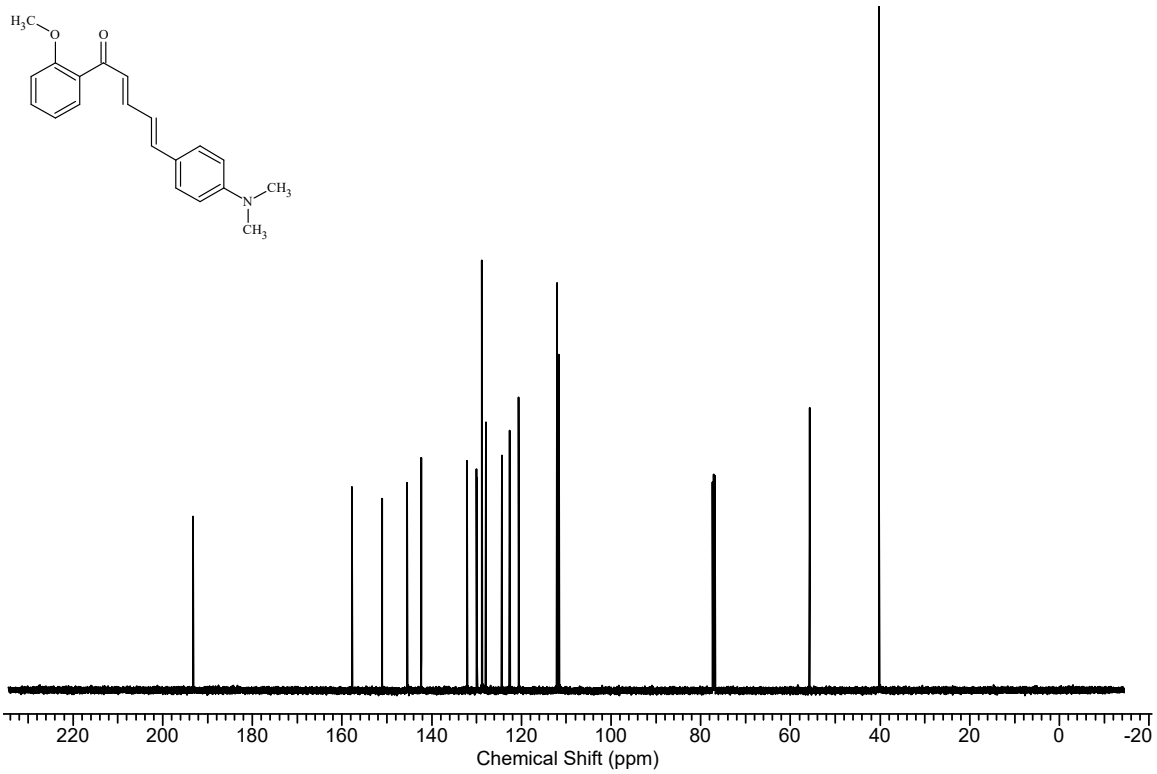

Figure S4. ^{13}C NMR of **1b** (125 MHz, $CDCl_3$) δ 193.2, 157.8, 151.0, 145.5, 142.4, 132.1, 130.0, 129.9, 128.8, 127.9, 124.3, 122.6, 120.6, 112.0, 111.6, 55.7, 40.2 ppm.

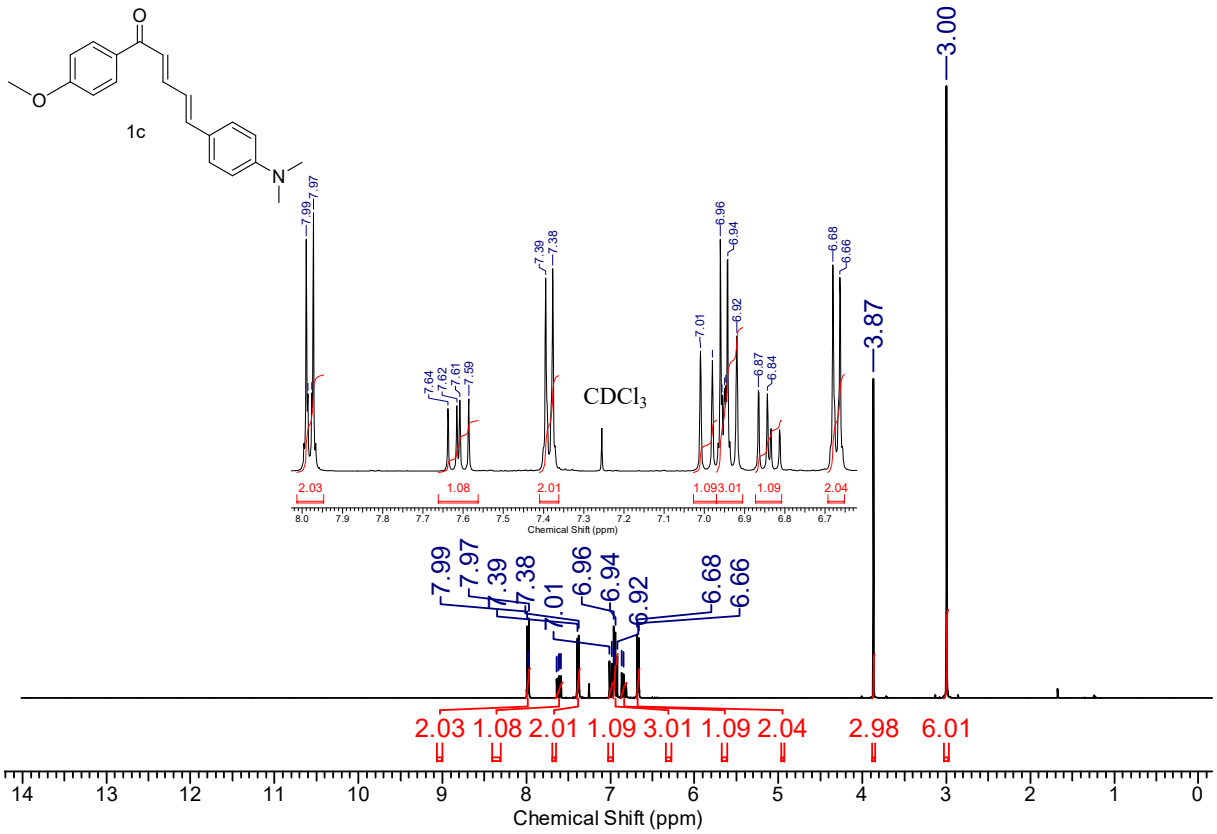

Figure S5. ^{1}HNMR of **1c** (500MHz, $CDCl_3$). δ 7.99-7.97 (d, J = 8.80 Hz, 2H), 7.64-7.59 (dd, J = 14.51, 11.25 Hz, 1H), 7.39-7.38 (d, J = 8.80 Hz, 2H), 7.01-6.98 (d. J = 14.67 Hz, 1H), 6.96-6.92 (m, 3H), 6.87-6.81 (dd, J = 15.06, 11.25 Hz, 1H), 6.68-6.66 (d, J = 8.80 Hz, 2H), 3.87 (s, 3H, OMe) 3.00 (s, 6H, NMe_2).

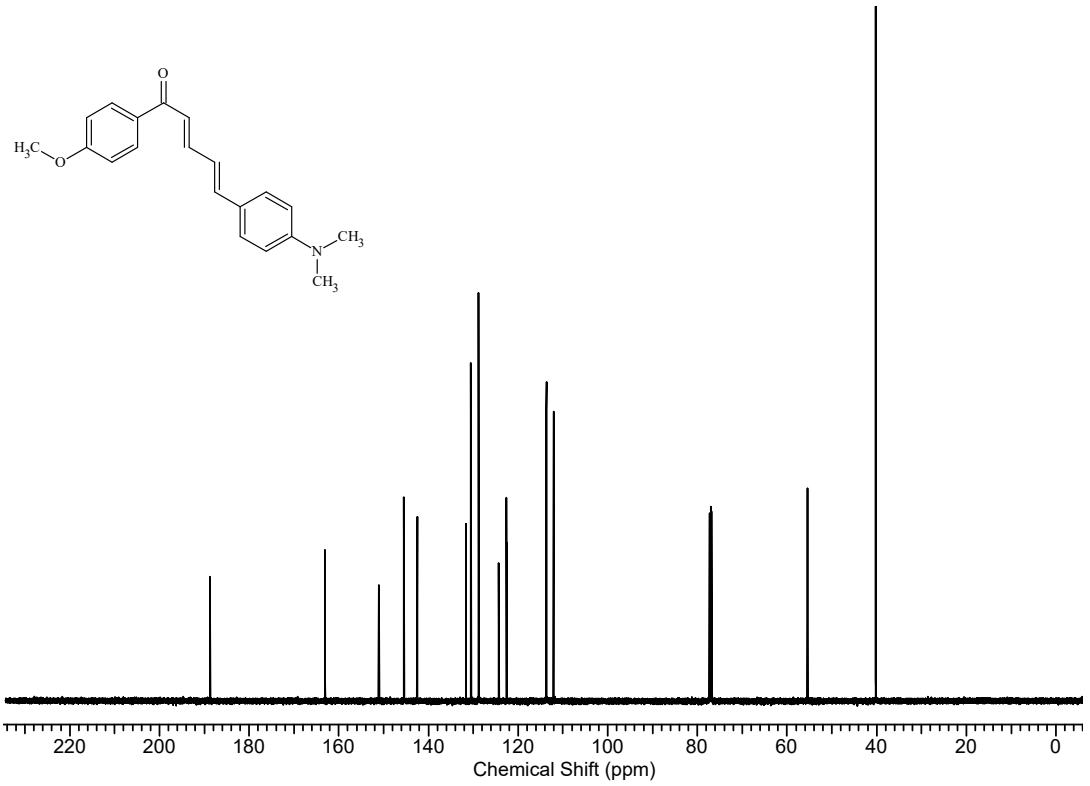

Figure S6. ^{13}C NMR of **1c** (125 MHz, $CDCl_3$) δ 188.7, 163.0, 151.0, 145.5, 142.5, 131.6, 130.5, 128.8, 124.3, 122.6, 113.7, 112.1, 55.4, 40.2 ppm.

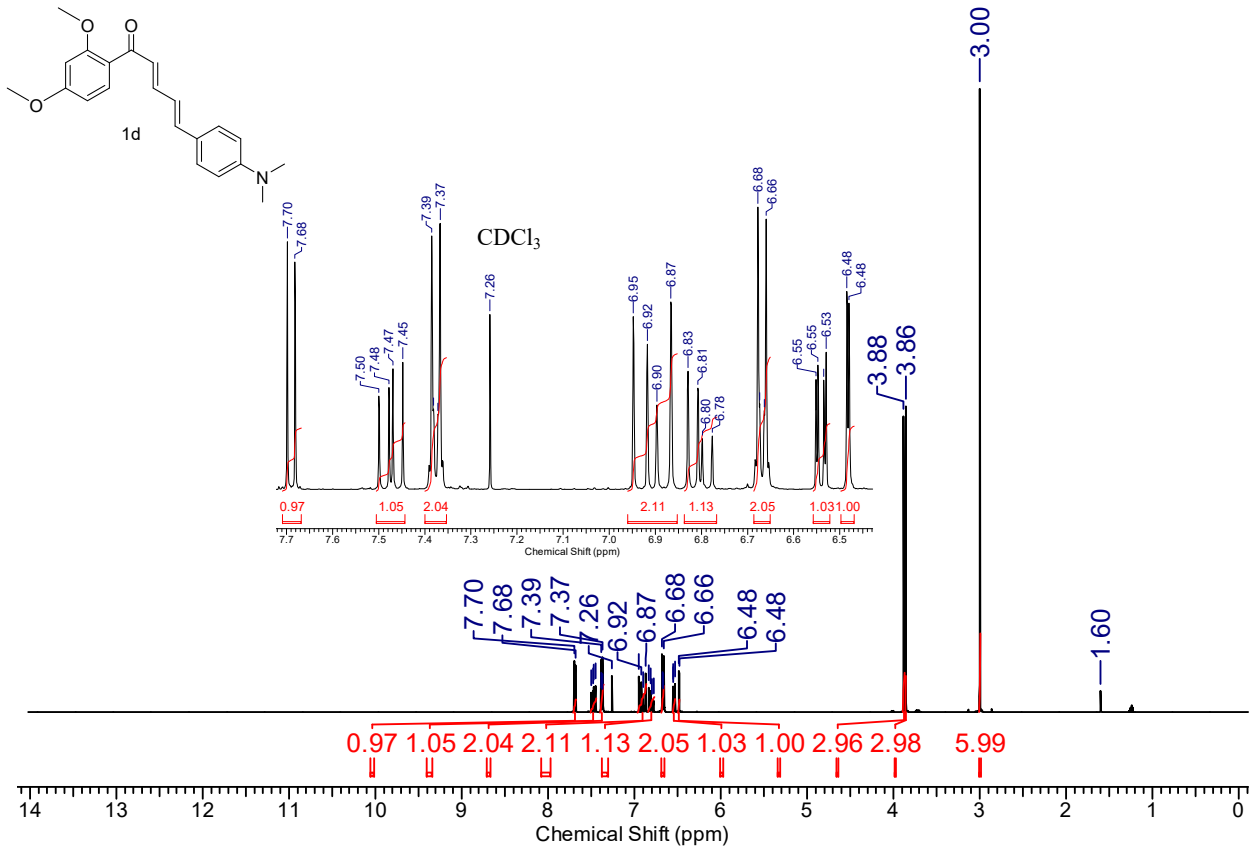

Figure S7. ^{1}HNMR of **1d** (500MHz, $CDCl_3$). δ 7.70-7.68 (d, J = 8.31 Hz, 1H) 7.50-7.45 (dd, J = 15.09, 10.76 Hz, 1H), 7.39-7.37 (d, J = 9.29 Hz, 2H), 6.95-6.87 (m, 2H), 6.83-6.78 (dd, J = 15.09, 10.76 Hz, 1H) 6.68-6.66 (d, J = 8.80 Hz, 2H), 6.55-6.53 (dd, J = 8.70, 1.96 Hz, 1H), 6.48 (d, J = 2.45 Hz, 1H), 3.88 (s, 3H, 2'-OMe), 3.86 (s, 3H, 4'-OMe), 3.00 (s, 6H, NMe_2).

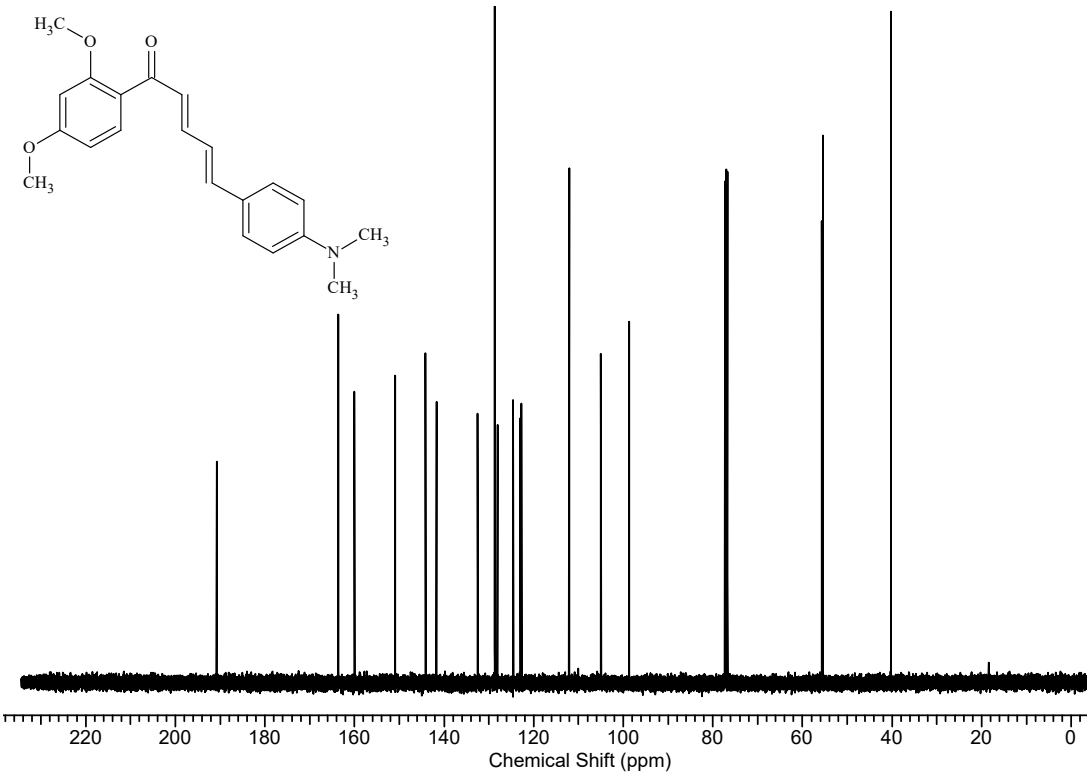

Figure S8. ^{13}C NMR of **1d** (125 MHz, $CDCl_3$) δ 190.8, 163.7, 160.1, 150.9, 144.1, 141.7, 132.5, 128.7, 128.1, 124.6, 123.0, 122.7, 112.1, 105.0, 98.7, 55.7, 55.5, 40.2 ppm.

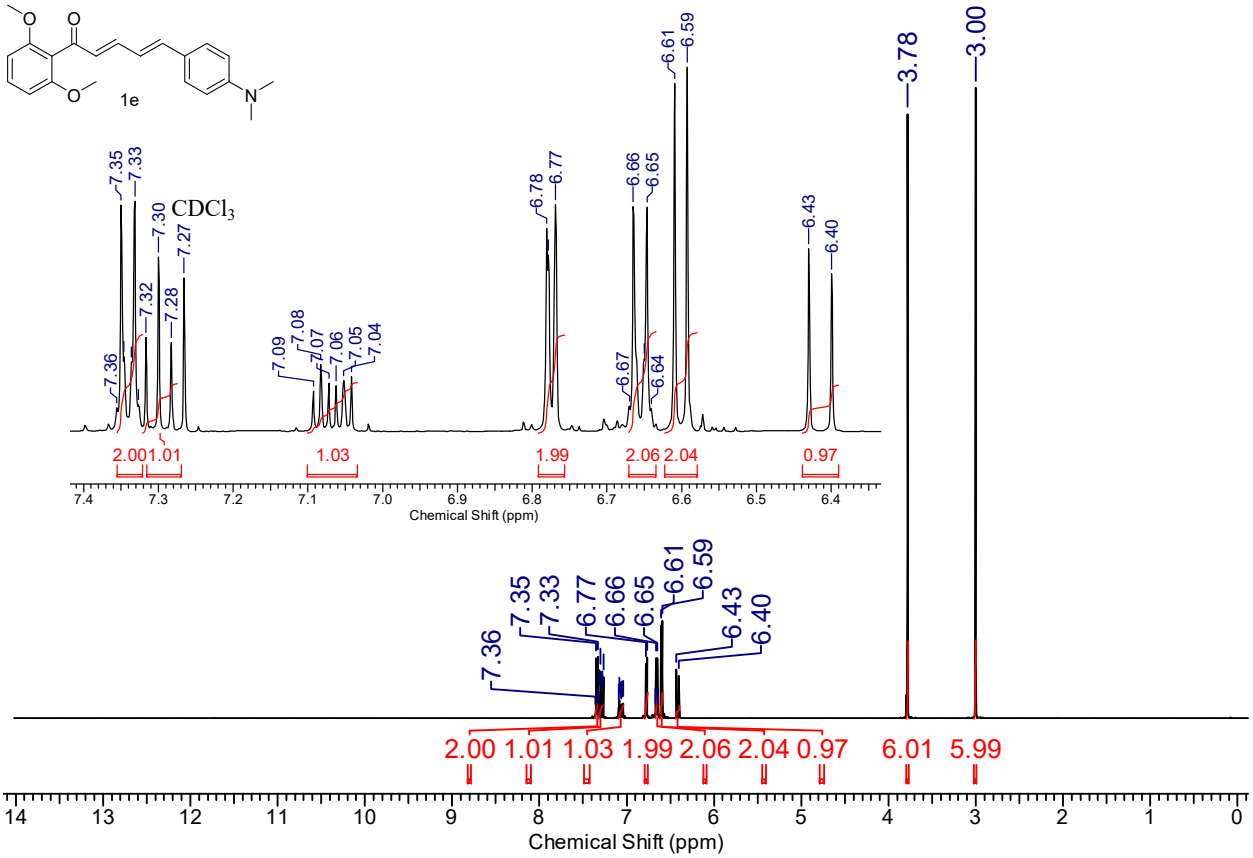

Figure S9. ^{1}HNMR of **1e** (500MHz, $CDCl_3$). δ 7.35-7.33 (d, J = 9.29 Hz, 2H), 7.30 (t, J = 8.31 Hz, 1H), 7.09-7.04 (dt, J = 15.16, 4.89 Hz, 1H), 6.78-6.77 (d, J = 4.89 Hz, 2H), 6.66-6.65 (d, J = 9.29 Hz, 2H), 6.61-6.59 (d, J = 8.31 Hz, 2H), 6.43-6.40 (d, J = 15.16 Hz, 1H), 3.78 (s, 6H, OMe), 3.00 (s, 6H, NMe2).

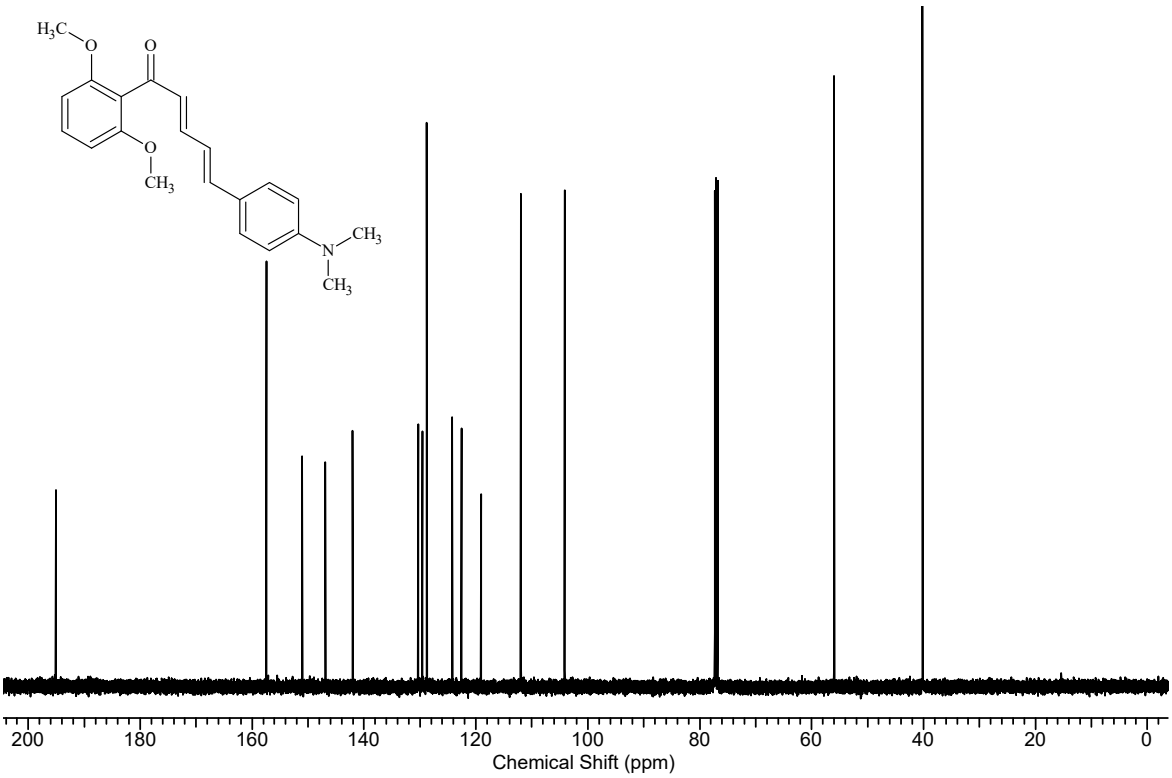

Figure S10. ^{13}C NMR of **1e** (125 MHz, $CDCl_3$) δ 195.1, 157.5, 151.0, 146.9, 142.0 130.3, 129.6, 128.8, 124.4, 122.6, 119.0, 112.0, 104.1, 56.0, 40.2 ppm.

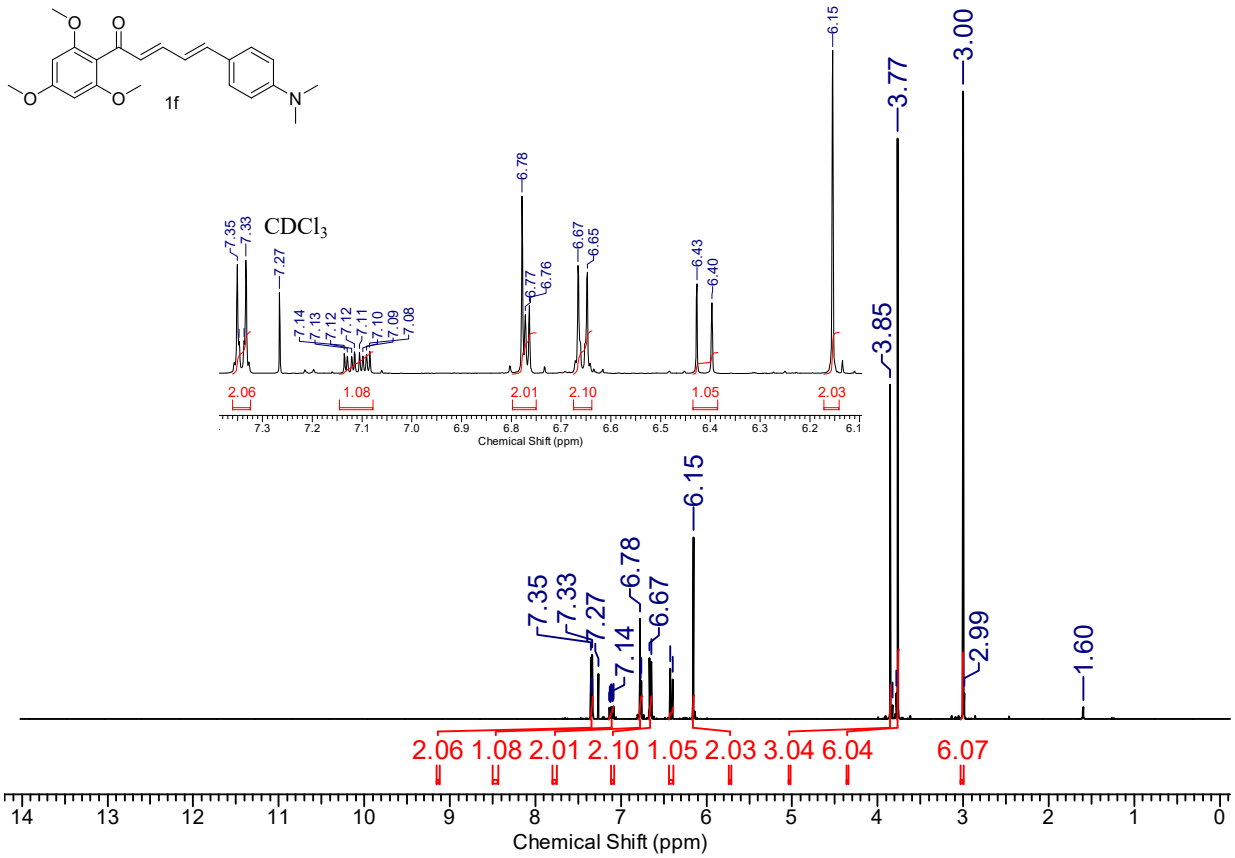

Figure S11. ^{1}HNMR of **1f** (500MHz, $CDCl_3$). δ 7.35-7.33 (d, J = 8.80 Hz, 2H), 7.14-7.08 (qd, J = 15.16, 7.29, 2.93 Hz, 1H), 6.78 (m, 2H), 6.67-6.65 (d, J = 9.29 Hz, 2H), 6.43-6.40 (d, J = 15.16 Hz, 1H), 6.15 (s, 2H), 3.85 (s, 3H, OMe), 3.77 (s, 6H, OMe), 3.00 (s, 6H, NMe_2).

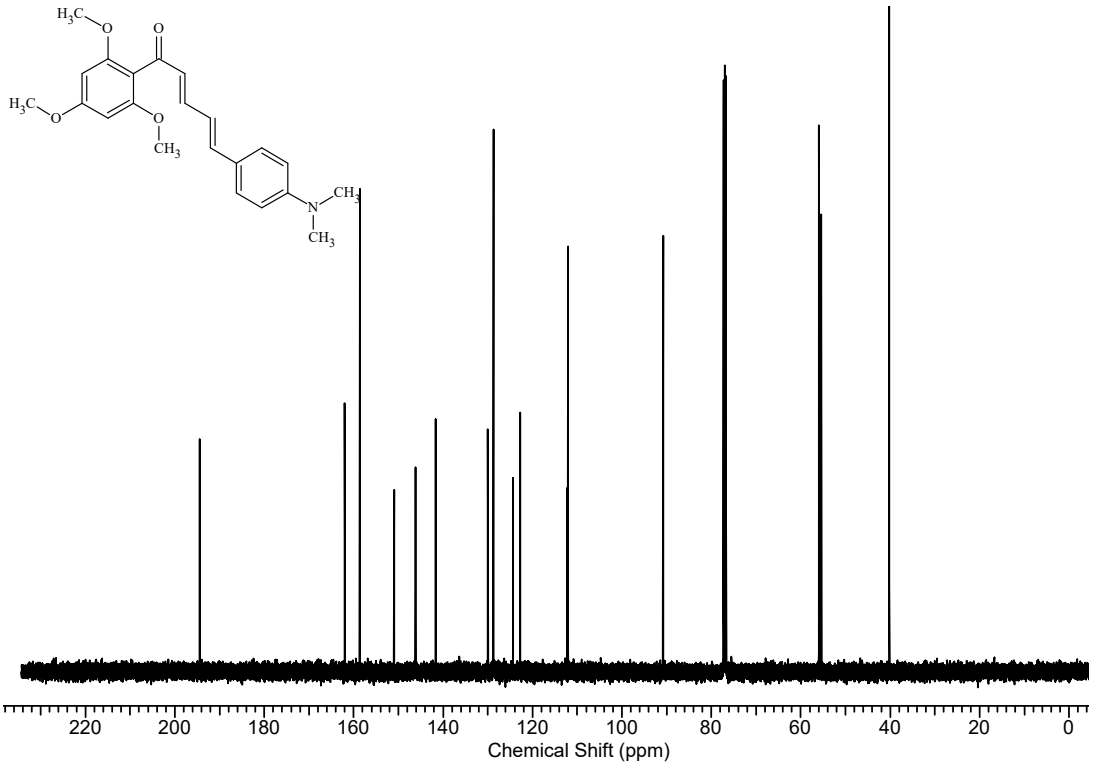

Figure S12. ^{13}C NMR of **1f** (125 MHz, $CDCl_3$) δ 194.4, 162.0, 158.6, 151.0, 146.2, 141.7, 130.0, 128.7, 124.4, 122.7, 112.3, 112.0, 90.8, 55.9, 55.9, 40.2 ppm.

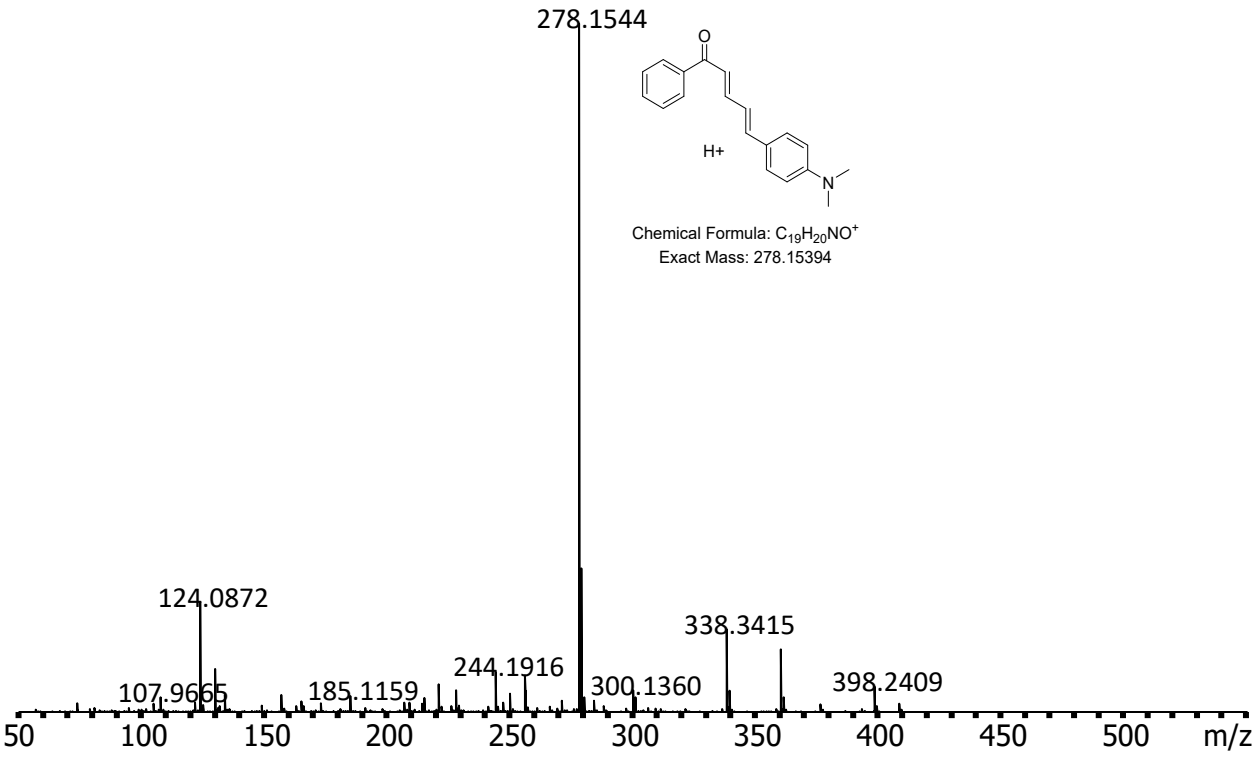

Figure S13. ESI-MS of **1a** in ACN.

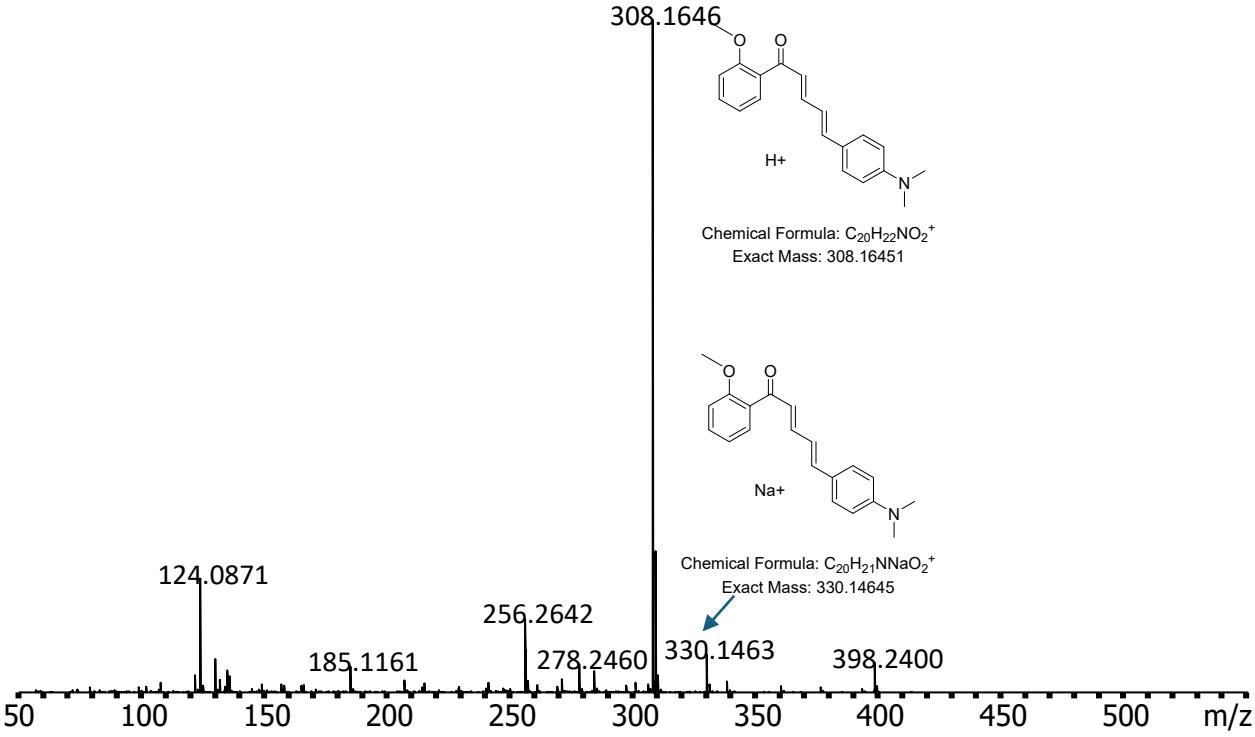

Figure S14. ESI-MS of **1b** in ACN.

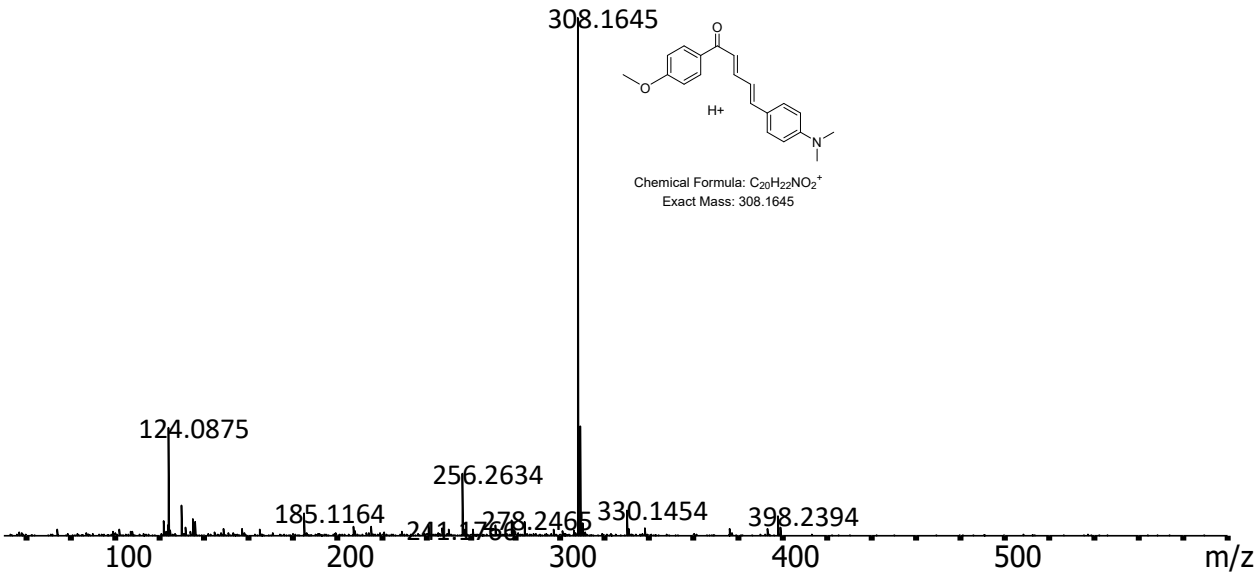

Figure S15. ESI-MS of **1c** in ACN.

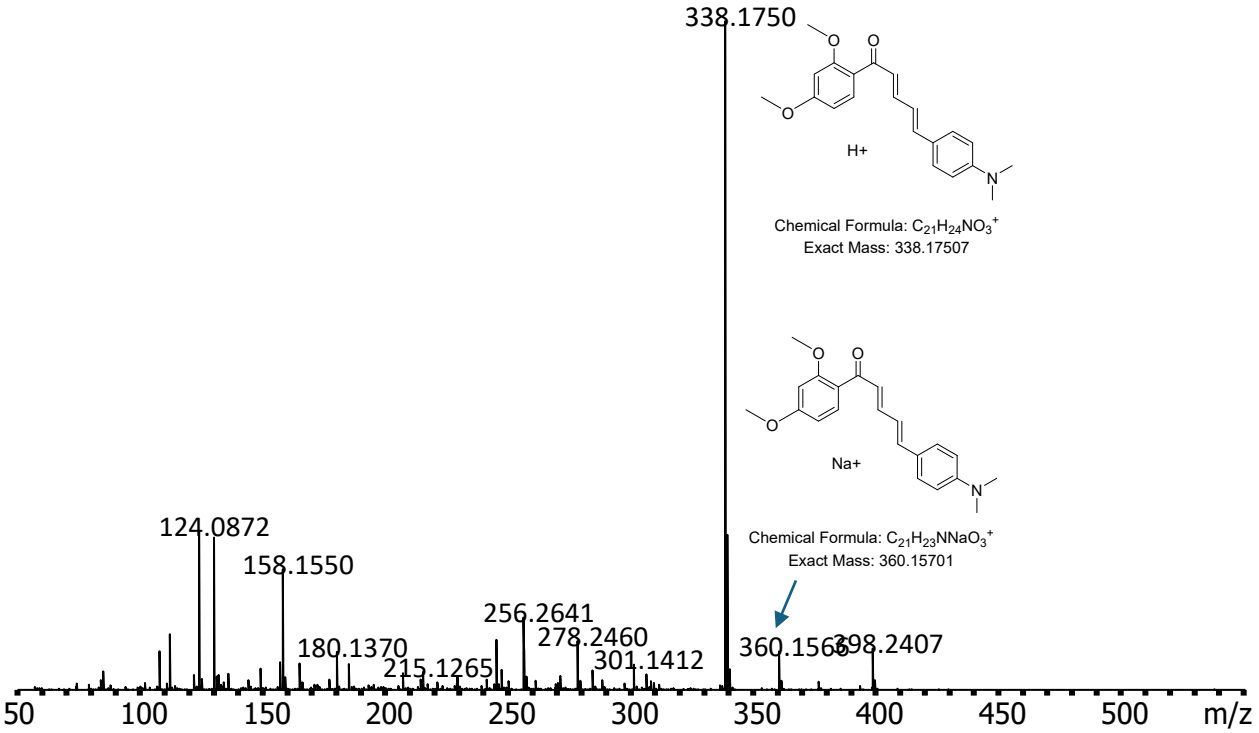

Figure S16. ESI-MS of **1d** in ACN.

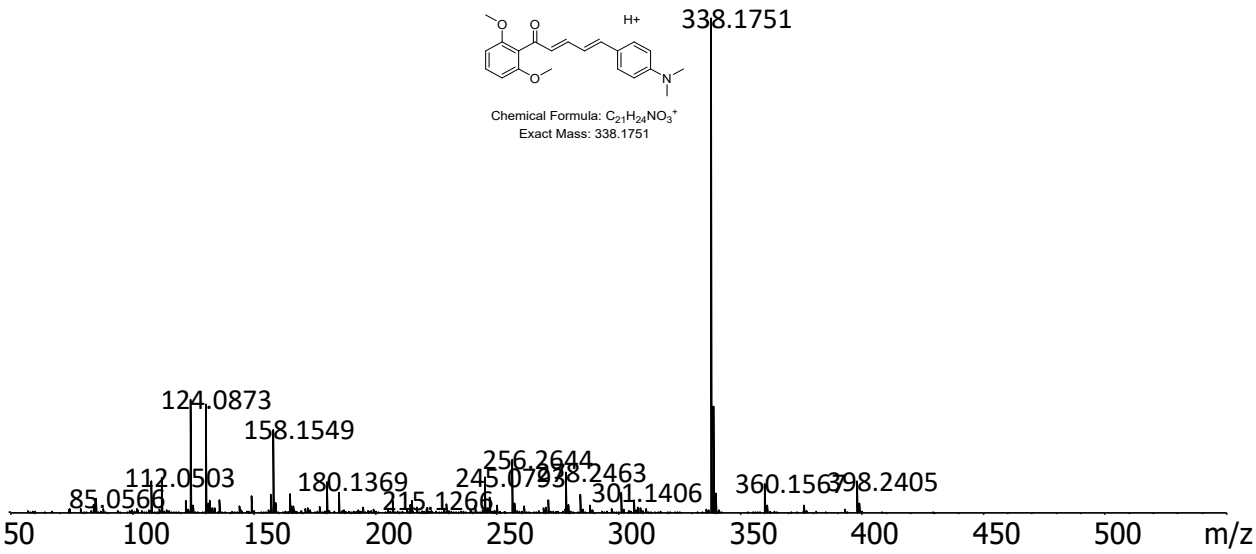

Figure S17. ESI-MS of **1e** in ACN.

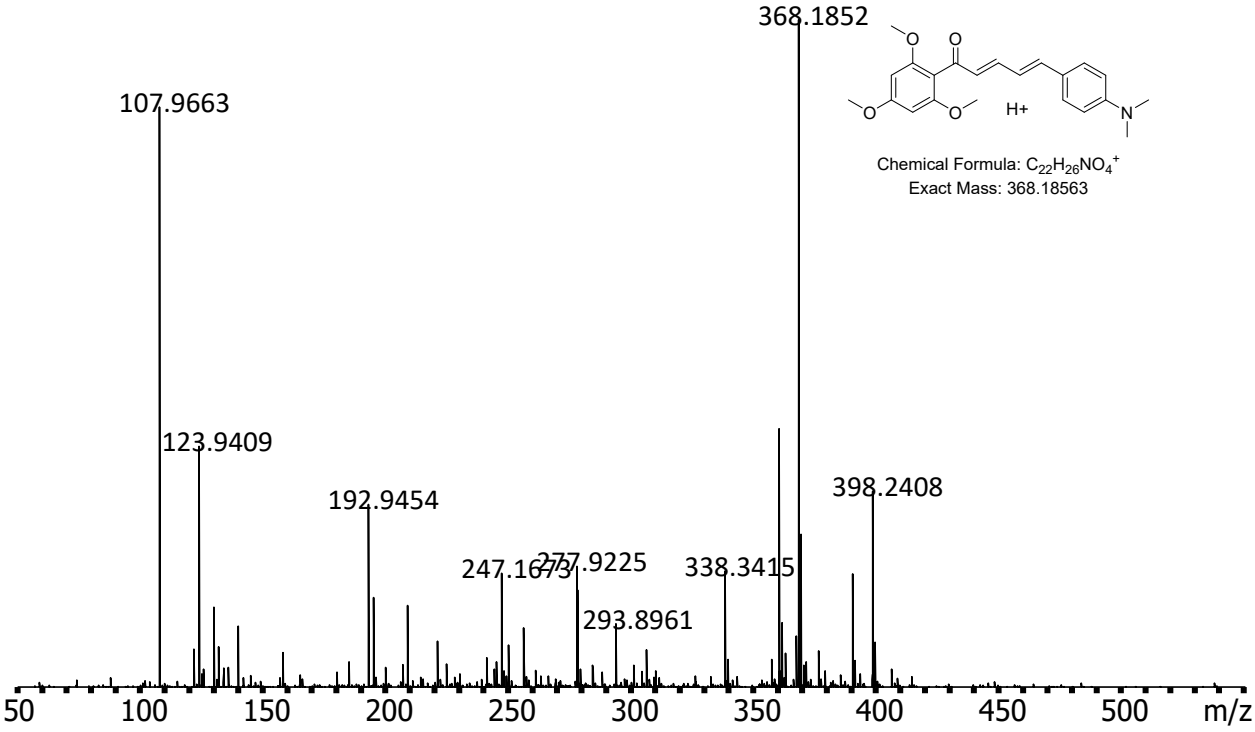

Figure S18. ESI-MS of **1f** in ACN.

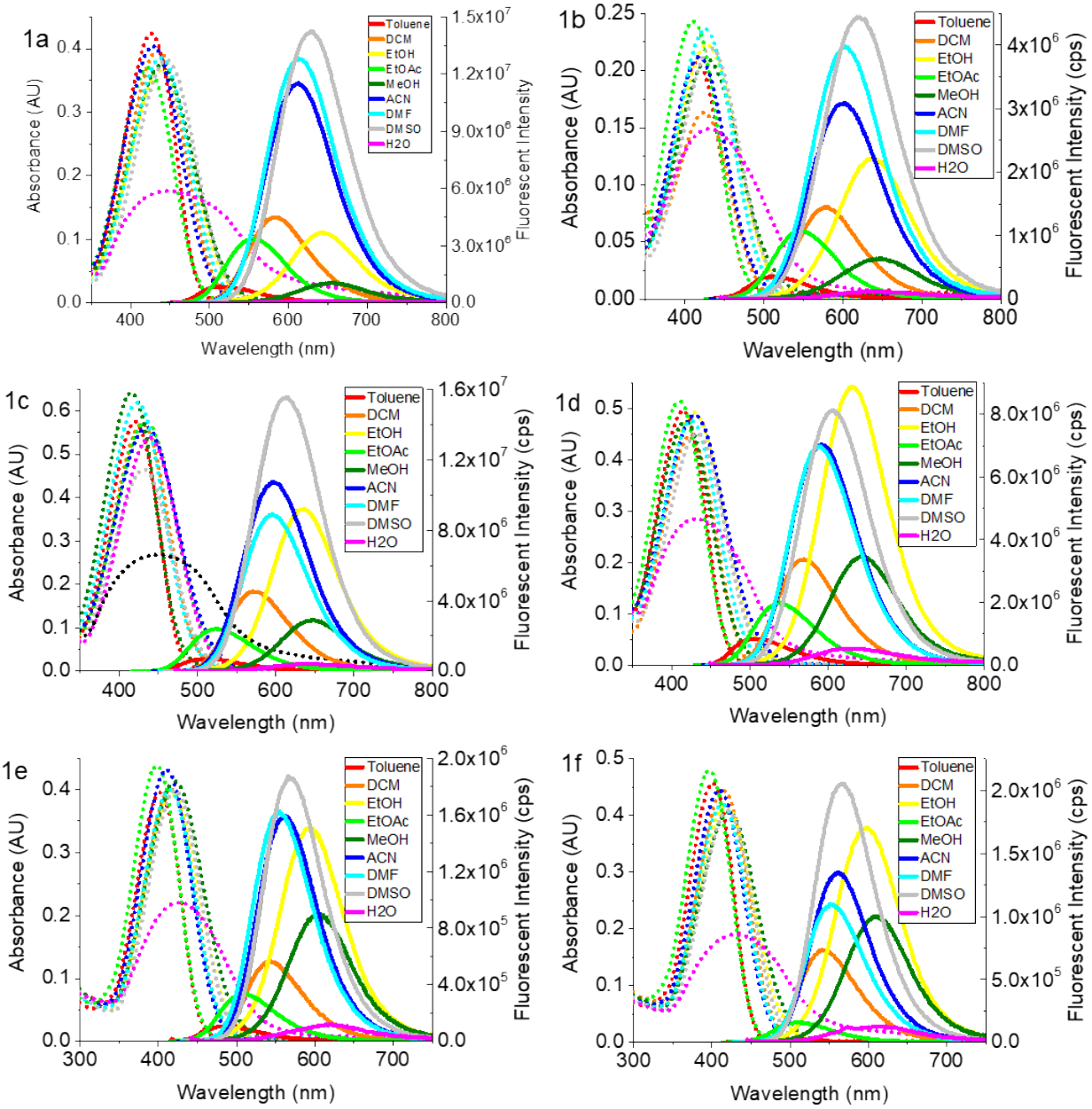

Figure S19. Absorbance (dotted lines) and emission (solid lines) spectra of **1a–1f** at 10 μM in various organic solvents.

Table S1. Optical properties of **1a–1f** (10 μM) in various organic solvents.

Compound	Solvent	λ_{abs} (nm)	λ_{Em} (nm)	Φ_{fl}	ε ($M^{-1}cm^{-1}$)	Δλ (nm)
1a	Toluene	426	518	0.019	42,405	92
	DCM	437	586	0.119	39,753	149
	EtOH	438	645	0.084	36,598	207
	EtOAc	424	556	0.059	36,985	132
	MeOH	440	658	0.032	37,435	218
	ACN	429	612	0.301	40,383	183
	DMF	439	615	0.346	38,587	176
	DMSO	446	630	0.354	38,239	184
	H2O	445	640	0.009	17,640	195
1b	Toluene	415	510	0.019	41,370	95
	DCM	424	580	0.063	32,640	156
	EtOH	429	640	0.128	44,492	211
	EtOAc	410	547	0.050	48,632	137
	MeOH	430	650	0.041	41,916	220
	ACN	418	601	0.160	42,406	183
	DMF	426	604	0.204	47,226	178
	DMSO	433	621	0.283	44,010	188
	H2O	435	635	0.008	29,790	200
1c	Toluene	424	510	0.015	57,497	86
	DCM	429	572	0.117	56,978	143
	EtOH	435	637	0.176	57,452	202
	EtOAc	415	547	0.038	64,171	132
	MeOH	433	647	0.044	56,180	214
	ACN	424	598	0.205	61,902	174
	DMF	432	595	0.178	46,521	163
	DMSO	440	615	0.301	53,814	175
	H2O	455	641	0.007	26,874	186
1d	Toluene	415	508	0.019	49,618	93
	DCM	424	570	0.076	44,579	146
	EtOH	428	630	0.213	49,250	202
	EtOAc	412	536	0.035	51,499	124
	MeOH	419	646	0.075	47,530	227
	ACN	428	593	0.130	48,661	165
	DMF	425	589	0.124	47,585	164
	DMSO	433	607	0.245	45,116	174
	H2O	432	630	0.008	28,522	198
1e	Toluene	402	486	0.004	39,553	84
	DCM	417	543	0.015	40,106	126
	EtOH	420	595	0.038	39,232	175
	EtOAc	399	507	0.007	43,796	108
	MeOH	420	605	0.021	41,336	185
	ACN	410	562	0.029	43,126	152
	DMF	416	555	0.032	39,975	139
	DMSO	421	570	0.053	39,908	149
	H2O	430	622	0.003	22,039	192
1f	Toluene	400	492	0.001	45,722	92
	DCM	415	542	0.013	44,496	127
	EtOH	418	600	0.048	41,842	182
	EtOAc	397	510	0.004	48,052	113
	MeOH	422	610	0.024	40,685	188
	ACN	408	561	0.026	44,458	153
	DMF	414	552	0.027	42,076	138
	DMSO	420	568	0.048	40,963	148
	H2O	433	613	0.004	19,081	180

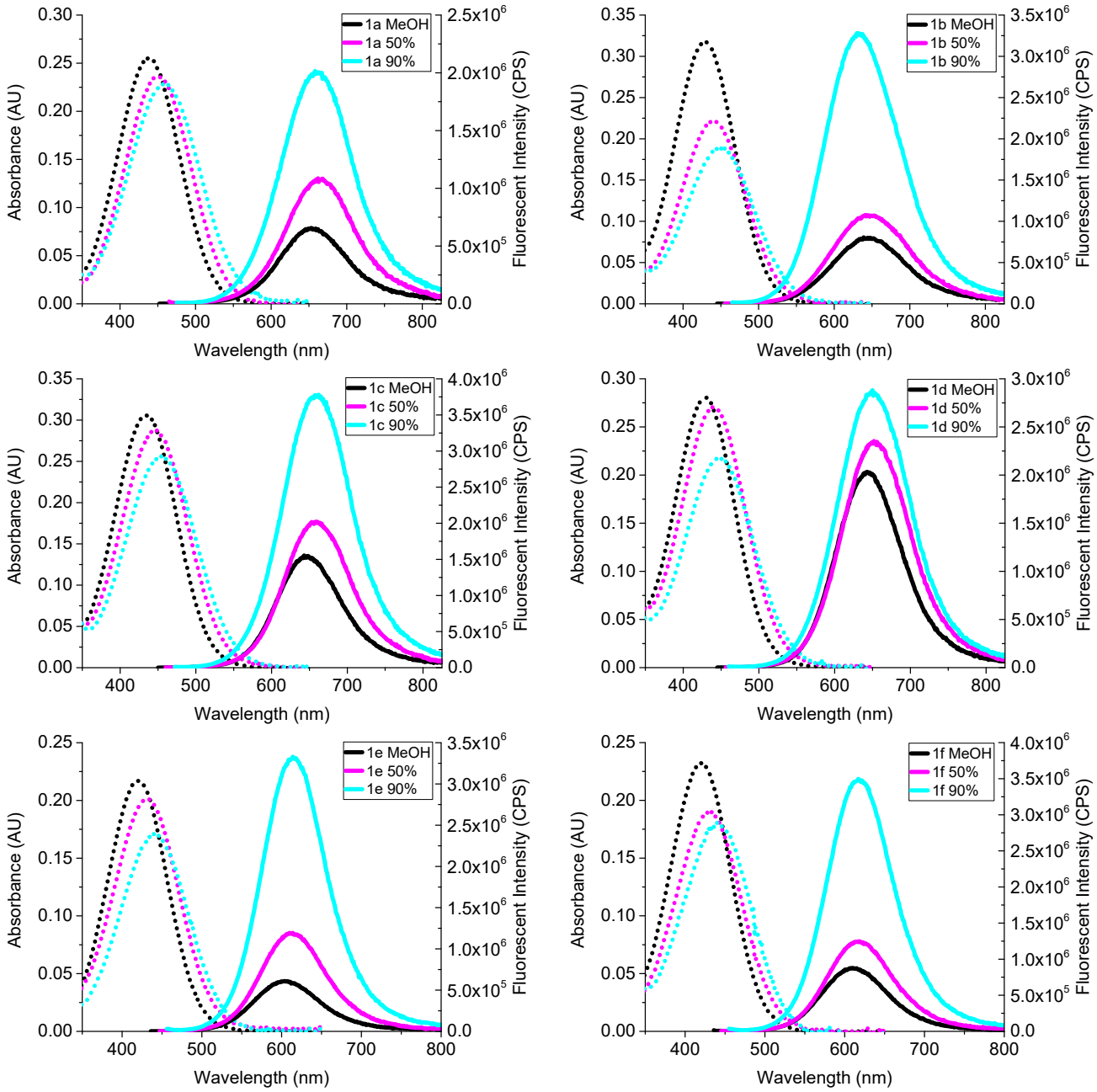

Figure S20. Absorption (dotted lines, left axis) and fluorescence emission spectra (solid lines, right axis) of compounds **1a–1f** (5μM) recorded in MeOH and MeOH/glycerol mixtures of increasing viscosity (50% and 90% v/v glycerol).

Table S2. Photophysical properties of **1a**-**1f** (5 μM) in 90:10 glycerol/MeOH.

Compound	λ_{abs} (nm)	λ_{Em} (nm)	Φ_{fl}	Δλ (nm)
1a	457	661	0.146	204
1b	450	633	0.202	183
1c	455	660	0.214	205
1d	449	650	0.209	201
1e	441	615	0.222	174
1f	441	617	0.235	176

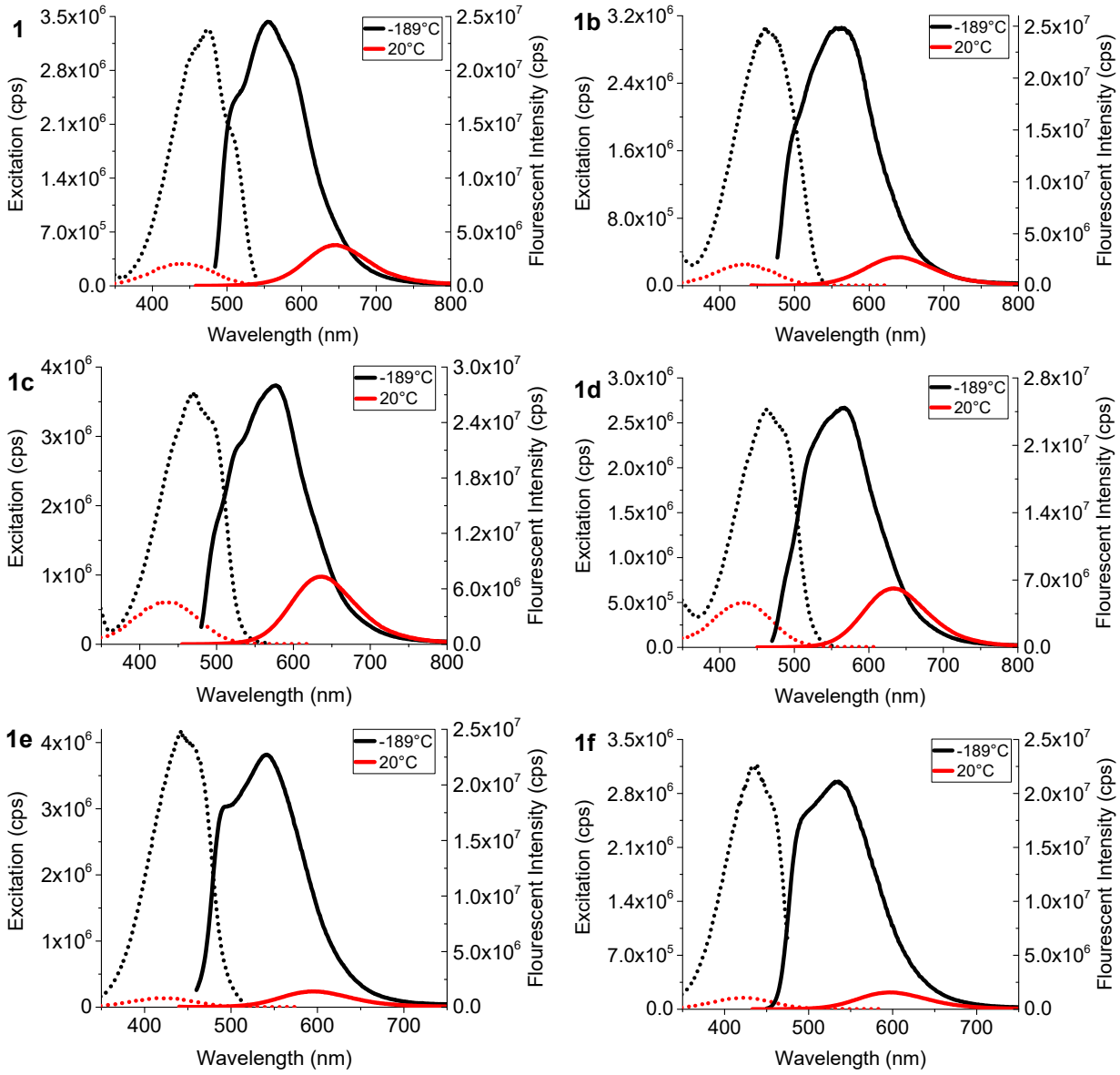

Figure S21. Excitation (dotted lines) and emission (solid lines) of **1a-1f** in EtOH at -189°C (black) and room temperature (red).

Table S3. Fluorescence lifetimes (τ_1, τ_2), pre-exponential amplitude contributions (α_1, α_2), intensity-weighted average lifetimes ($\bar{\tau}$), and goodness-of-fit values (χ^2) for compounds **1a–1f** measured in solution at room temperature. All decay profiles were best fit using a bi-exponential model.

Compound	Solvent	τ_1 (ns)	α_1 (%)	τ_2 (ns)	α_2 (%)	$\bar{\tau}$ (ns)	χ^2
1a	DCM	0.453	31	0.635	69	0.59	1.21
	EtOH	0.180	10	0.434	90	0.41	1.18
	ACN	0.690	10	1.285	90	1.23	1.21
1b	DCM	0.197	21	0.564	79	0.52	1.12
	EtOH	0.586	13	0.694	87	0.69	1.03
	ACN	0.207	7	1.091	93	1.07	1.04
1c	DCM	0.344	74	0.560	26	0.41	1.16
	EtOH	0.166	5	0.793	95	0.79	1.02
	ACN	0.504	9	0.913	91	0.90	1.11
1d	DCM	0.312	86	0.588	14	0.34	1.17
	EtOH	0.601	11	0.969	89	0.96	1.20
	ACN	0.438	15	0.801	85	0.76	1.22
1e	DCM	0.054	51	0.110	49	0.083	0.93
	EtOH	0.250	72	0.450	28	0.32	0.92
	ACN	0.170	95	0.600	5	0.19	0.89
1f	DCM	0.051	52	0.110	48	0.081	0.99
	EtOH	0.280	47	0.500	47	0.39	1.19
	ACN	0.150	83	0.320	17	0.17	1.07

Table S4. X-Ray crystallography information for **1a-1f**.

Identification code	**1a**	**1b**	**1c**	**1d**	**1e**	**1f**
CCDC	2497318	2497319	2497320	2497321	2497322	2497323
Empirical formula	$C_{19}H_{19}NO$	$C_{20}H_{21}NO_2$	$C_{21}H_{22}Cl_3NO_2$	$C_{21}H_{23}NO_3$	$C_{21}H_{23}NO_3$	$C_{22}H_{25}NO_4$
Formula weight	277.35	307.38	426.74	337.40	337.40	367.43
Temperature	100(2) K	100(2) K	100(2) K	100(2) K	100(2) K	100(2) K
Wavelength	0.71073 Å	0.71073 Å	0.71073 Å	0.71073 Å	0.71073 Å	0.71073 Å
Crystal system	Monoclinic	Orthorhombic	Orthorhombic	Monoclinic	Orthorhombic	Monoclinic
Space group	$P2_1/c$	Pbca	$Pna2_1$	$P2_1/c$	$Pna2_1$	$P2_1/n$
Unit cell dimensions	a = 14.669(4) Å α= 90°.	a = 7.727(2) Å α= 90°.	a = 10.719(3) Å α= 90°.	a = 12.280(2) Å α= 90°.	a = 6.4711(10) Å α= 90°.	a = 7.8584(13) Å α= 90°.
	b = 10.904(3) Å β= 102.022(9)°	b = 13.395(4) Å β= 90°.	b = 26.404(6) Å β= 90°.	b = 13.278(3) Å β= 90.359(8)°.	b = 37.579(6) Å β= 90°.	b = 7.1808(14) Å β= 95.044(6)°.
	c = 9.588(3) Å γ = 90°.	c = 31.495(9) Å γ = 90°.	c = 7.2837(18) Å γ = 90°.	c = 11.121(2) Å γ = 90°.	c = 7.3111(10) Å γ = 90°.	c = 35.233(7) Å γ = 90°.
Volume	1499.9(6) $Å^3$	3259.8(16) $Å^3$	2061.5(9) $Å^3$	1813.4(6) $Å^3$	1777.9(5) $Å^3$	1980.5(6) $Å^3$
Z	4	8	4	4	4	4
Density (calculated)	1.228 Mg/m^3	1.253 Mg/m^3	1.375 Mg/m^3	1.236 Mg/m^3	1.261 Mg/m^3	1.232 Mg/m^3
Absorption coefficient	0.075 mm^{-1}	0.080 mm^{-1}	0.461 mm^{-1}	0.082 mm^{-1}	0.084 mm^{-1}	0.084 mm^{-1}
F(000)	592	1312	888	720	720	784
Crystal size	0.318 x 0.292 x 0.234 mm^3	0.446 x 0.312 x 0.228 mm^3	0.252 x 0.236 x 0.086 mm^3	0.608 x 0.159 x 0.140 mm^3	0.633 x 0.427 x 0.150 mm^3	0.532 x 0.492 x 0.226 mm^3
Theta range for data collection	1.419 to 24.857°.	2.936 to 26.458°.	2.050 to 26.453°.	1.658 to 26.458°.	2.168 to 28.264°.	2.321 to 28.466°.
Index ranges	-17<=h<=17, -12<=k<=12, -11<=l<=11	-9<=h<=9, -16<=k<=16, -39<=l<=39	-13<=h<=13, -29<=k<=32, -9<=l<=9	-15<=h<=15, -16<=k<=16, -13<=l<=13	-8<=h<=8, -50<=k<=50, -6<=l<=9	-10<=h<=10, -9<=k<=9, -47<=l<=47
Reflections collected	27525	107477	23412	31563	37508	86772
Independent reflections	2575 [R(int) = 0.0623]	3350 [R(int) = 0.0864]	4162 [R(int) = 0.0675]	3724 [R(int) = 0.0597]	3984 [R(int) = 0.0921]	4970 [R(int) = 0.0809]
Completeness to theta = 24.857°	99.0 %	99.6 %	99.9 %	99.9 %	99.9 %	99.7 %
Absorption correction	Semi-empirical	Semi-empirical	Semi-empirical	Semi-empirical	Semi-empirical	Semi-empirical
Refinement method	Full-matrix least-squares on F^2	Full-matrix least-squares on F^2	Full-matrix least-squares on F^2	Full-matrix least-squares on F^2	Full-matrix least-squares on F^2	Full-matrix least-squares on F^2
Data / restraints / parameters	2575 / 0 / 237	3350 / 0 / 211	4162 / 1 / 247	3724 / 0 / 230	3984 / 1 / 230	4970 / 0 / 249
Goodness-of-fit on F^2	1.127	1.099	1.173	1.065	1.043	1.052
Final R indices [I>2sigma(I)]	R1 = 0.0523, wR2 = 0.1170	R1 = 0.0414, wR2 = 0.0969	R1 = 0.0402, wR2 = 0.0749	R1 = 0.0409, wR2 = 0.0938	R1 = 0.0468, wR2 = 0.1033	R1 = 0.0472, wR2 = 0.1111
R indices (all data)	R1 = 0.0655, wR2 = 0.1247	R1 = 0.0512, wR2 = 0.1051	R1 = 0.0627, wR2 = 0.0893	R1 = 0.0556, wR2 = 0.1028	R1 = 0.0655, wR2 = 0.1162	R1 = 0.0622, wR2 = 0.1239
Largest diff. peak and hole	0.197 and -0.195 e.$Å^{-3}$	0.239 and -0.185 e.$Å^{-3}$	0.310 and -0.330 e.$Å^{-3}$	0.174 and -0.197 e.$Å^{-3}$	0.210 and -0.203 e.$Å^{-3}$	0.289 and -0.236 e.$Å^{-3}$

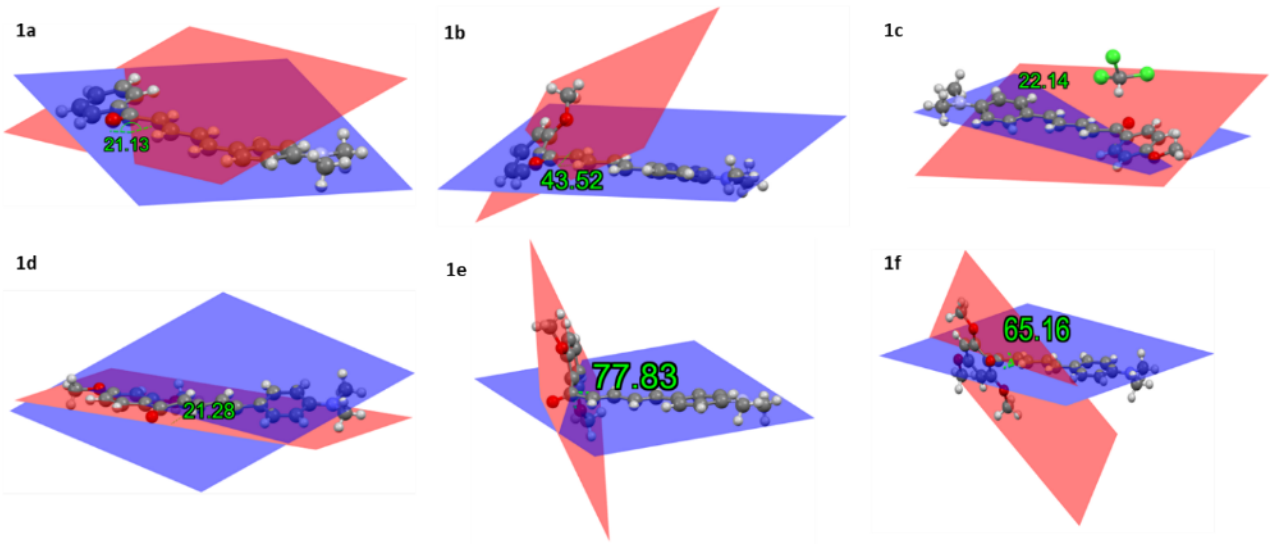

Figure S22. Interplanar angles from the crystal stuctures of 1a-1f.

Mercury was used to generate the red and blue reference planes shown above. The red plane was defined using only the carbon atoms of the A-ring, excluding methoxy substituents, while the blue plane was defined by the unsaturated carbon atoms spanning the enone linkage between the carbonyl group and the B-ring. The resulting interplanar angles therefore quantify the degree of torsional deviation between the A-ring and the conjugated backbone.

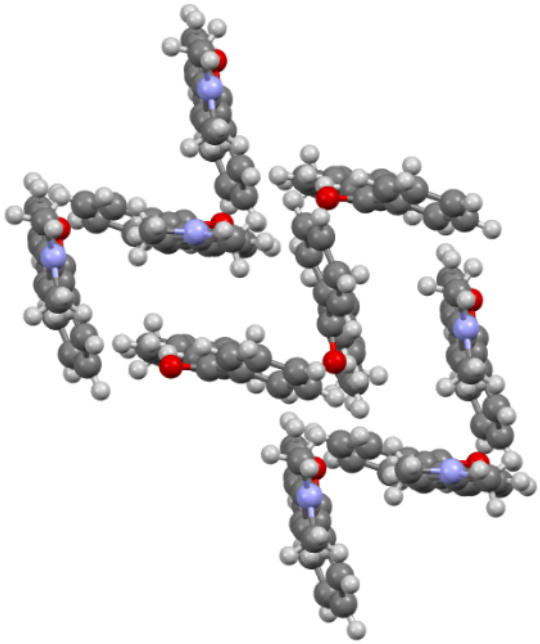

Figure S23. Crystal packing of chalcone **1a** illustrating the orthoganal packing behavior between the dimer-like complexes.

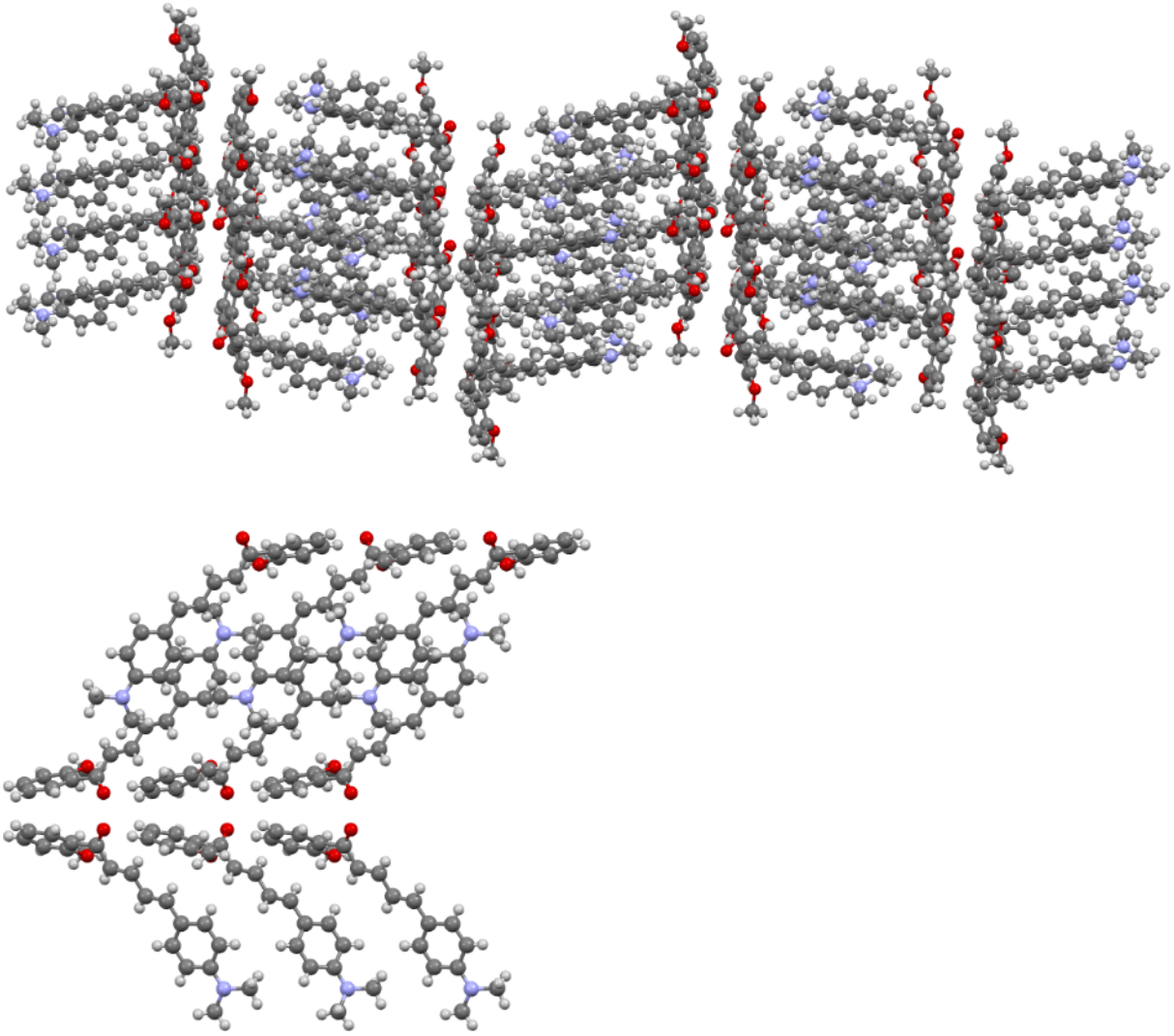

Figure S24. Top, crystal packing of **1b** along the "b" axis in a 2x2x2 matrix. Bottom, alternative view showing the nonparrallel stacking of the A-rings in **1b**.

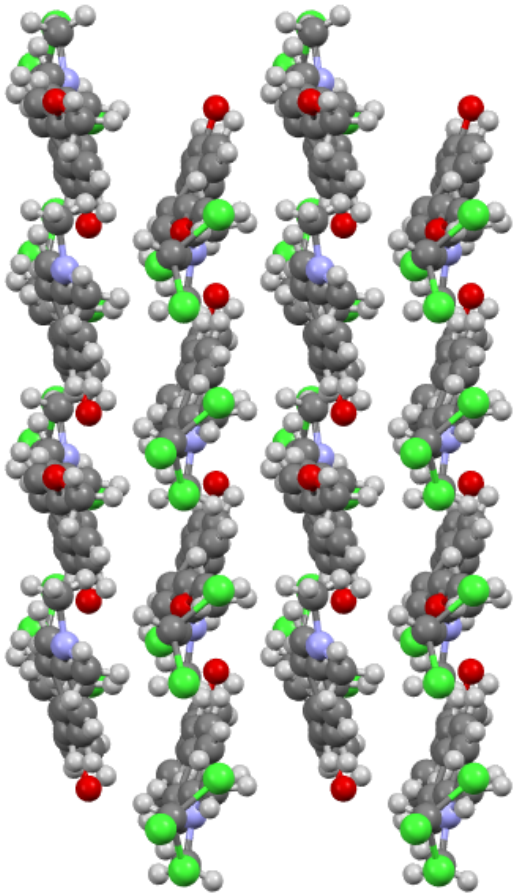

Figure S25. Crystal packing of **1c** along the b-axis. Chloroform molecules shown to highlight hydrogen bond formation to carbonyl unit of each chromophore.

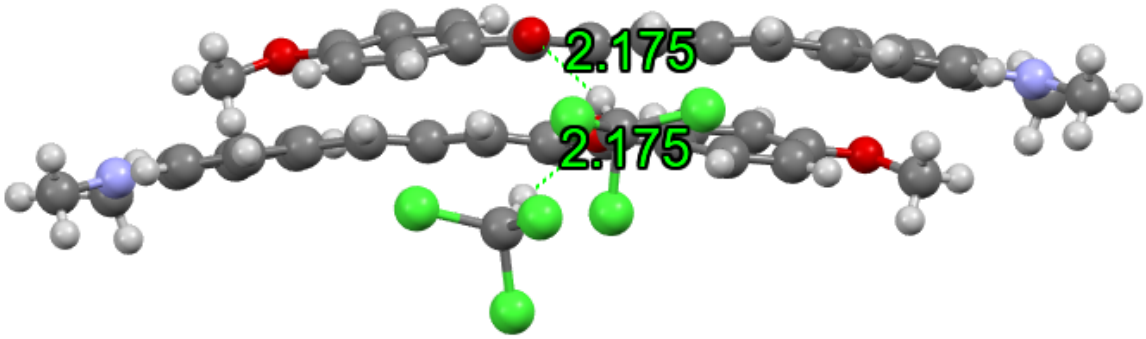

Figure S26. Crystal packing of **1c** showing intermolecular hydrogen bond distance (Å) between co-crystallized chloroform and the carbonyl oxygen.

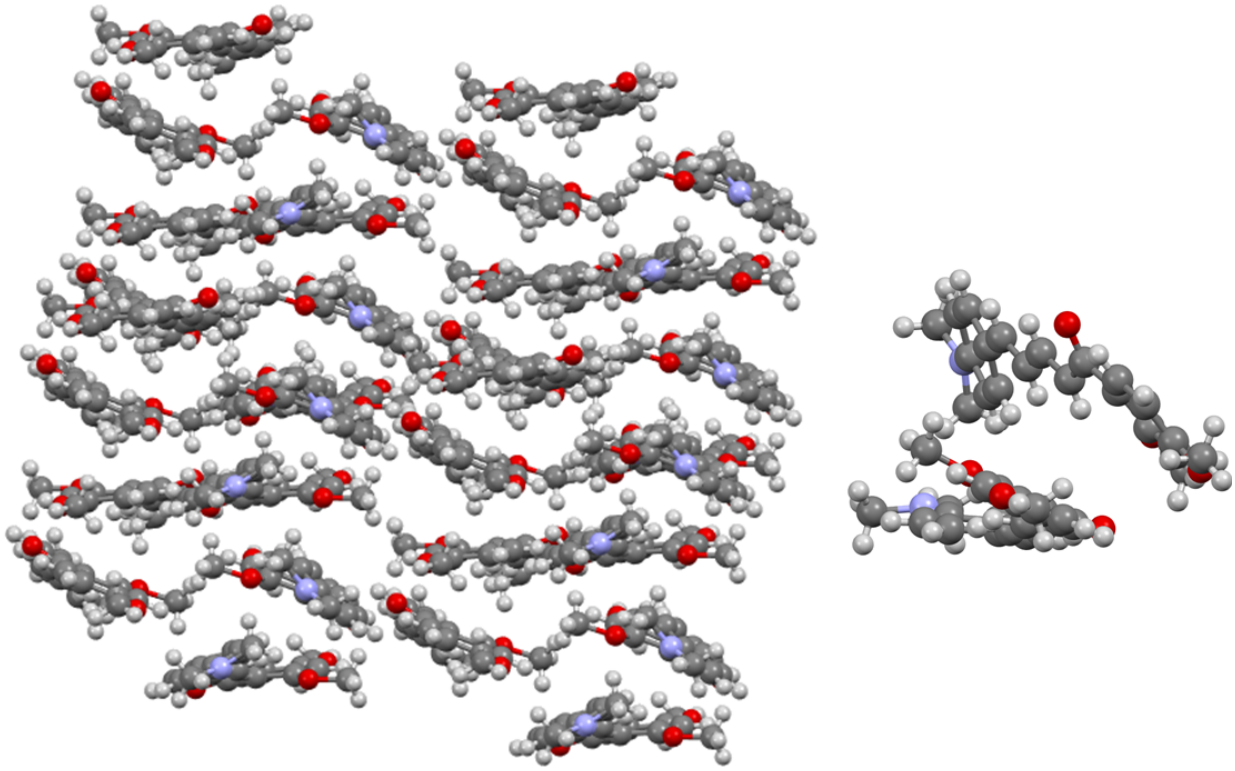

S27. Crystal packing of **1d** with an isolated view of the planar offset between two molecules on the right.

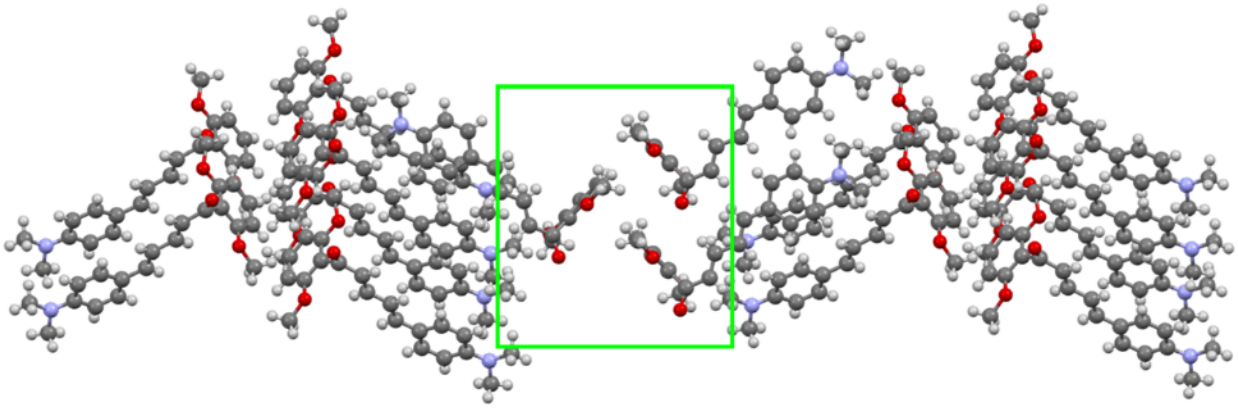

Figure S28**.** Crystal packing of **1e** illustrating an edge-to-face arrangement of the A-rings, highlighted in green.

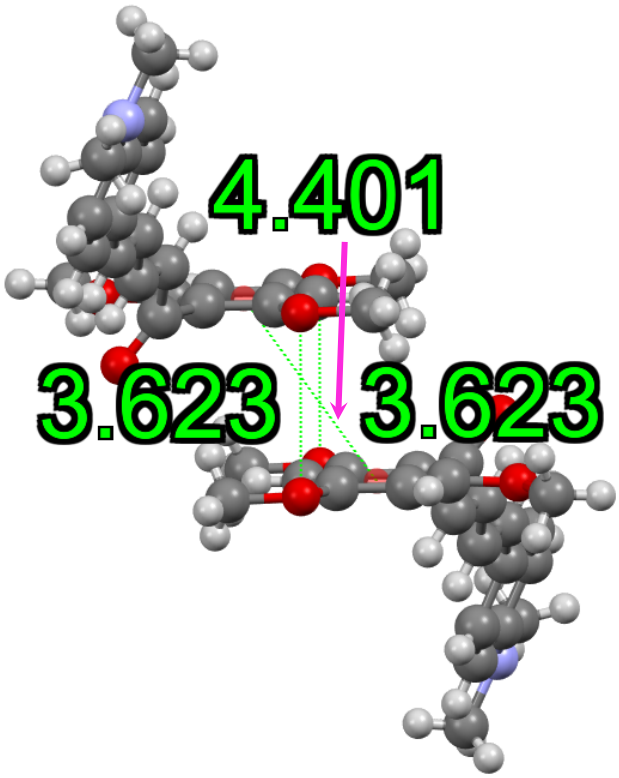

Figure S29. Crystal packing of **1f** illusstrating the slip-stacked packing behavior. The centroid distances is 4.401 Å and indicated by the pink arrow. The interatomic distance between the 2 vertically aligned ortho and para methoxy groups is identical at 3.623 Å.

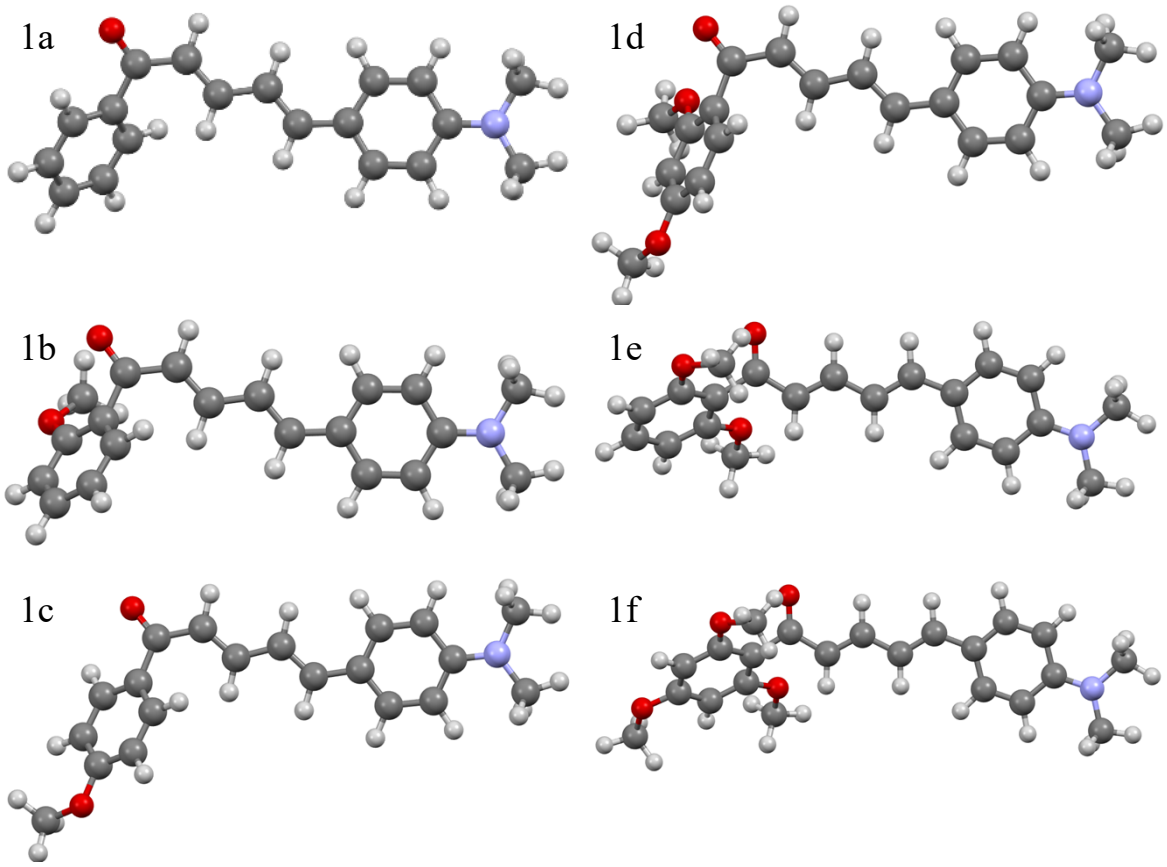

Figure S30. Optimized ground state geometries of series of **1a-1f**.

Table S5. Comparison of Kohn–Sham energy gaps and computed TD-DFT optical transition energies in DCM.

Compound	ε(HOMO) (eV)	ε(LUMO) (eV)	ΔE_{ks}[a] (eV)	λ_{abs} (nm)	E_{abs}[b] (eV)	λ_{em} (nm)	E_{em}[b] (eV)
1a	−5.272	−2.273	2.999	446	2.780	510	2.431
1b	−5.320	−2.080	3.240	440	2.818	501	2.475
1c	−5.239	−2.198	3.041	443	2.799	505	2.455
1d	−5.241	−2.168	3.073	435	2.850	495	2.505
1e	−5.239	−2.300	2.939	456	2.719	516	2.403
1f	−5.211	−2.244	2.967	456	2.719	478	2.594

[a] ΔE_{ks} = ε(LUMO) − ε(HOMO). Kohn–Sham orbital energies were obtained from optimized S_0 geometries (B3LYP/6-311G(d), PCM-DCM).
[b] Optical transition energies were converted using $E(\text{eV}) = 1239.84/\lambda(\text{nm})$.

Table S6. Comparison of experimental and calculated TD-DFT optical transition energies in DCM.

Compound	Exp λ_{abs} (nm)	Exp E_{abs} (eV)	Exp λ_{em} (nm)	Exp E_{em} (eV)	Calcd λ_{abs} (nm)	Calcd E_{abs} (eV)	Calcd λ_{em} (nm)	Calcd E_{em} (eV)
1a	437	2.84	586	2.12	446	2.78	510	2.43
1b	424	2.92	580	2.14	440	2.82	501	2.48
1c	429	2.89	572	2.17	443	2.80	505	2.46
1d	424	2.92	570	2.18	435	2.85	495	2.51
1e	417	2.97	543	2.28	456	2.72	516	2.40
1f	415	2.99	542	2.29	456	2.72	478	2.59

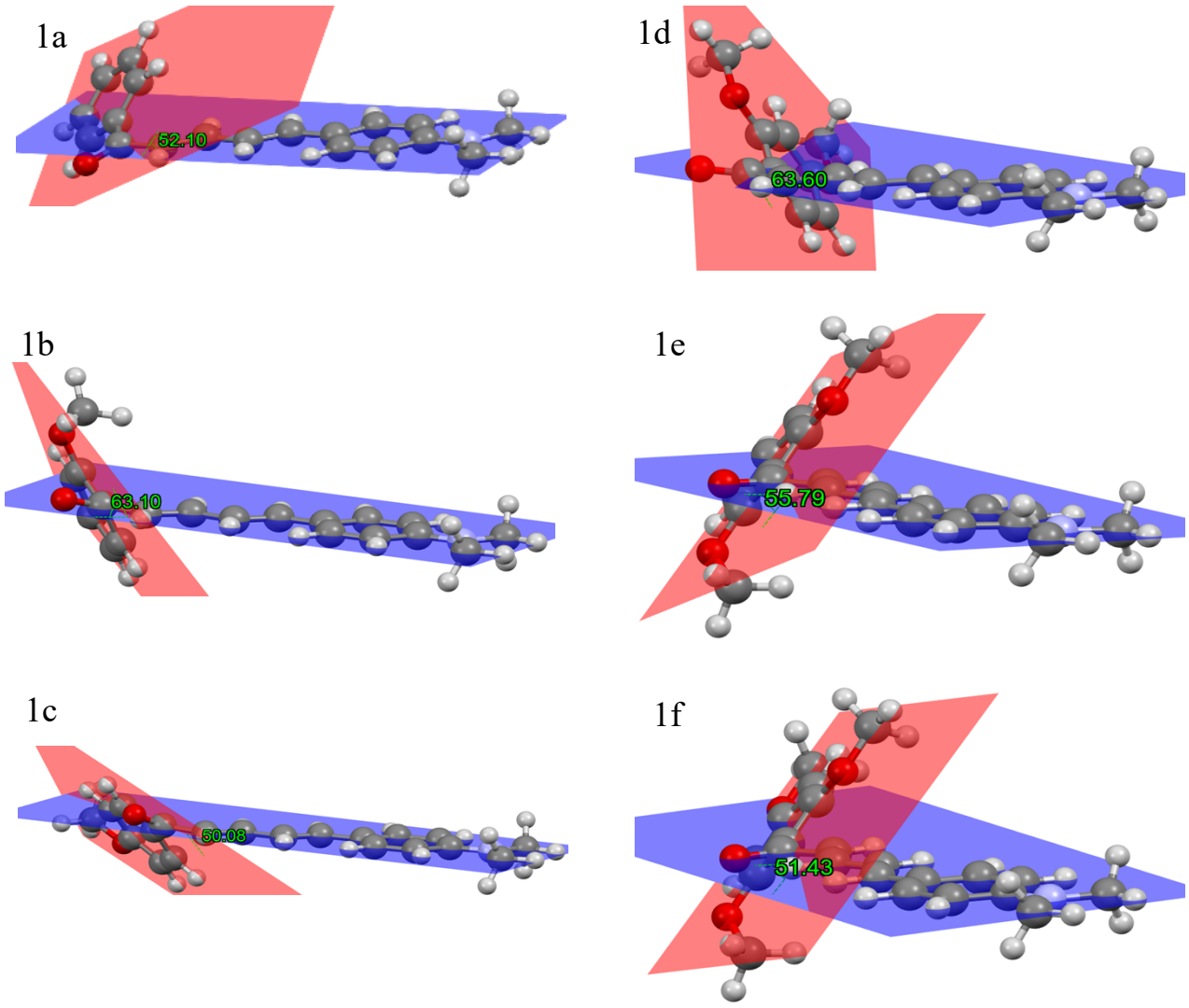

Figure S31. Interplanar angles of the A-ring (red) and B-ring (blue) for series of **1a-1f** using the optimized ground state geometries .

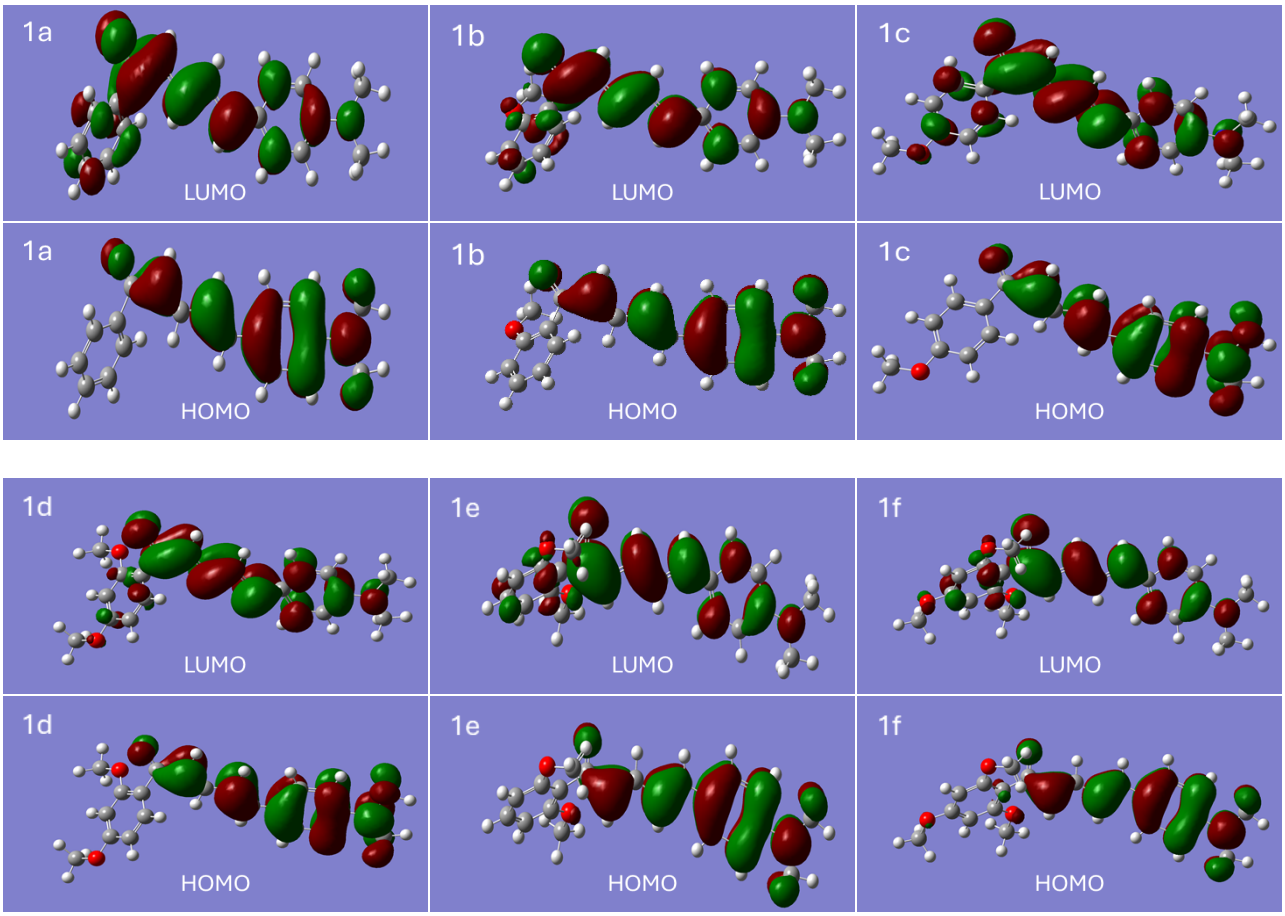

Figure S32. HOMO-LUMO diagrams of **1a-1f** calculated using B3LYP/6-311G(d) in DCM.